



Persistent organic pollutants in global surface soils: Distributions and fractionations



Yi-Fan Li ^{a, b, c, d, *}, Shuai Hao ^{a, b, c}, Wan-Li Ma ^{a, b, c, **}, Pu-Fei Yang ^{a, b, c}, Wen-Long Li ^e,
Zi-Feng Zhang ^{a, b, c}, Li-Yan Liu ^{a, b, c}, Robie W. Macdonald ^{f, g}

^a International Joint Research Center for Persistent Toxic Substances (IJRC-PTS), State Key Laboratory of Urban Water Resource and Environment, Harbin Institute of Technology, Harbin, 150090, China

^b International Joint Research Center for Arctic Environment and Ecosystem (IJRC-AEE), Polar Academy, Harbin Institute of Technology (PA-HIT), Harbin, 150090, China

^c Heilongjiang Provincial Key Laboratory of Polar Environment and Ecosystem (HPKL-PEE), Harbin, 150090, China

^d IJRC-PTS-NA, Toronto, ON, M2J 3N8, Canada

^e College of the Environment and Ecology, Xiamen University, Xiamen, China

^f Institute of Ocean Sciences, Department of Fisheries and Oceans, P.O. Box 6000, Sidney, BC, V8L 4B2, Canada

^g Centre for Earth Observation Science, University of Manitoba, Winnipeg, R3T 2N2, Canada

ARTICLE INFO

Article history:

Received 25 October 2022

Received in revised form

30 July 2023

Accepted 17 August 2023

Keywords:

POPs

Primary and secondary sources

Primary and secondary emissions

Primary and secondary distribution patterns

Primary and secondary fractionations

ABSTRACT

The distribution and fractionation of persistent organic pollutants (POPs) in different matrices refer to how these pollutants are dispersed and separated within various environmental compartments. This is a significant study area as it helps us understand the transport efficiencies and long-range transport potentials of POPs to enter remote areas, particularly polar regions. This study provides a comprehensive review of the progress in understanding the distribution and fractionation of POPs. We focus on the contributions of four intermedia processes (dry and wet depositions for gaseous and particulate POPs) and determine their transfer between air and soil. These processes are controlled by their partitioning between gaseous and particulate phases in the atmosphere. The distribution patterns and fractionations can be categorized into primary and secondary types. Equations are developed to quantitatively study the primary and secondary distributions and fractionations of POPs. The analysis results suggest that the transfer of low molecular weight (LMW) POPs from air to soil is mainly through gas diffusion and particle deposition, whereas high molecular weight (HMW) POPs are mainly via particle deposition. HMW-POPs tend to be trapped near the source, whereas LMW-POPs are more prone to undergo long-range atmospheric transport. This crucial distinction elucidates the primary reason behind their temperature-independent primary fractionation. However, the secondary distribution and fractionation can only be observed along a temperature gradient, such as latitudinal or altitudinal transects. An animation is produced by a one-dimensional transport model to simulate conceptively the transport of CB-28 and CB-180, revealing the similarities and differences between the primary and secondary distributions and fractionations. We suggest that the decreasing temperature trend along latitudes is not the major reason for POPs to be fractionated into the polar ecosystems, but drives the longer-term accumulation of POPs in cold climates or polar cold trapping.

© 2023 The Author(s). Published by Elsevier B.V. on behalf of Chinese Society for Environmental Sciences, Harbin Institute of Technology, Chinese Research Academy of Environmental Sciences. This is an open access article under the CC BY-NC-ND license (<http://creativecommons.org/licenses/by-nc-nd/4.0/>).

* Corresponding author. International Joint Research Center for Persistent Toxic Substances (IJRC-PTS), State Key Laboratory of Urban Water Resource and Environment, Harbin Institute of Technology, Harbin, 150090, Heilongjiang, China.

** Corresponding author. International Joint Research Center for Persistent Toxic Substances (IJRC-PTS), State Key Laboratory of Urban Water Resource and Environment, Harbin Institute of Technology, Harbin, 150090, China.

E-mail addresses: dr_li_yifan@163.com (Y.-F. Li), mawanli002@163.com (W.-L. Ma).

1. Introduction

Persistent organic pollutants (POPs) are persistent, bio-accumulative, and toxic in the environment, with a high potential to undergo long-range transport. The sources of POPs, resulting from their various uses, can be well depicted by their primary emission inventories with different spatial and temporal

resolutions. Global-scale gridded emission inventories are currently available for only a limited number of POP groups. The first published global-scale gridded emission inventory focused on hexachlorocyclohexanes (HCHs) [1,2], followed by polychlorinated biphenyls (PCBs) [3–5], endosulfan [6], polycyclic aromatic hydrocarbons (PAHs) [7], and polybrominated diphenyl ethers (PBDEs) [8]. The global latitudinal emission distributions of α -HCH from 1945 to 2010 and 22 PCB congeners from 1930 to 2000 are present in Figs. S1a and b, Supporting Information (SI), clearly showing a “global source region” (GSR) of α -HCH and PCBs within specific latitude bands, from 20° to 50° N for the former [1] and from 30° to 60° N for the latter [3–5].

In general, the sources of POPs can be divided into primary and secondary sources. Primary sources involve the direct application and/or emission of POPs into the environment during their use and production. On the other hand, secondary sources involve the later redistribution of POPs between air and soil/water. Following their initial release, POPs disperse through the air and accumulate in surface soils through wet and dry depositions, forming secondary sources in soil, which can be remobilized as secondary emissions to the atmosphere. Once released, POPs can spread globally, even reaching remote areas like the Arctic [9–11]. Among all pathways, air movement is considered the most significant and rapid route for the global transport of most POPs. Consequently, over time, surface soils have become the largest reservoir for historical emissions of POPs. Thus, the soil should be a more appropriate medium for studying the global distribution processes of POPs than the atmosphere [12]. Therefore, in this study, we focus on surface soil, although a few other matrices are also discussed under some circumstances.

Multiple research groups have reported distribution patterns of POPs in the soil and air attributed to various sources. The existence of an “urban pulse” was revealed by levels of PBDEs [13] and PCBs [14] in both air and soil on a transect across Birmingham City, the United Kingdom (UK). Concentrations were highest in the city center and decreased with increasing distance away from the city. This urban pulse was also observed with the air concentrations of PCBs [15] and PBDEs [16] in an urban–rural transect in the Toronto area, Canada. Furthermore, the urban pulse was observed for the air concentrations of several emerging flame retardants (EFRs) and PBDEs in Stockholm, Sweden [17], and PCBs in the soil of the Moscow region [18].

Like the urban pulse, a so-called “point pulse” of a POP can be formed near a specific point source, such as a manufactory or an e-waste site that emits this chemical. Several instances of point pulses have been documented in surface soils, demonstrating elevated concentrations of PCBs and polychlorinated dibenzo-p-dioxins and dibenzo-furans (PCDDs/Fs) near e-waste sites [19], dechloranes surrounding a dechlorane plus (DP) manufactory in China [20], PCBs around a municipal solid waste incinerator [21], PCBs away from three chemical manufactures [22], PBDEs and tetrabromobisphenol-A (TBBPA) around an e-waste site [23], brominated flame retardants (BFRs) surrounding two BFR plants [24], PCBs and PBDEs near an e-waste site [25], and PBDEs and novel brominated flame retardants (NBFRs) surrounding two e-waste recycling facilities [26]. These cases have displayed strong negative correlations between chemical concentrations and distance from the sources, indicating the presence of point pulse patterns.

For over two decades, a few large-scale studies have investigated POPs in the surface soils, aiming to better understand their distribution and fate along latitudinal and longitudinal transects [27–29]. The latitudinal distribution of PCBs was first investigated

by Meijer and co-workers in surface soils [27] and air [30] across a latitudinal transect, spanning from 50.6° to 75° N through the UK and Norway. Five years later, a study was carried out for examining the longitudinal distribution of PCBs in Chinese rural and background soil, spanning from 94° to 122° E [28]. Additionally, similar investigations were conducted for PBDEs [31] and NBFRs [32] in soil samples collected from five Asian countries.

The concept of fractionation of POPs was initially proposed by Wania and Mackay in 1993 [33,34], known as global or latitudinal fractionation. This concept suggests that highly persistent semi-volatile chemicals (SVOCs) can be enriched within spatial temperature gradients, occurring on latitudinal or vertical scales [12,33,34]. Several studies have sought evidence of global fractionation by studying spatial trends of POPs in different matrixes, such as soil [27,35], air [36], vegetation, and biota samples [37,38]. Following the publication by Meijer and co-workers on latitudinal fractionation, a longitudinal fractionation on a large scale was reported for PCBs in Chinese background/rural soils [28]. Subsequently, similar studies were conducted for PBDEs [31] and NBFRs [32] in soil samples from five Asian countries.

Latitudinal and longitudinal fractionations on lowlands are usually observed on large scales, global or continental. In 2004, a so-called “urban fractionation” was reported for PCBs in the air on a local scale (~75 km) along an urban–rural transect in Toronto, Canada, by Harner and co-workers [15]. Subsequently, a similar urban fractionation pattern was identified for PCBs in soil along an urban–rural transect in and around Shanghai, China [28]. Analogously to the urban fractionation but with a smaller scale, a “point source fractionation” pattern was observed for both BFRs and NBFRs in the soil near industrial and e-waste sites in China [31,32]. This was further investigated by examining novel and legacy BFRs in the surface soil surrounding two e-waste recycling facilities in Australia [26].

Based on the distinct characteristics of reported fractionation types in the existing literature, Li and co-workers categorized these fractionations into two groups: primary and secondary fractionations [39]. Primary fractionation of POPs arises from primary factors, such as their sources, physiochemical properties, and travel distances away from the sources. It is identified as a higher proportion of certain substances than others as the distance from the source increases. The absolute amounts of individual substances still show a primary distribution pattern. Secondary fractionation of POPs occurs due to secondary factors, with ambient temperature being a key consideration. This fractionation is characterized not only as an increasing proportion for certain compounds with increasing distance away from the sources but also displaying a secondary distribution pattern for at least one individual substance [40].

Here, we have reviewed the distribution and fractionation patterns of POPs in the surface soil with the following objectives: (1) to explore and define the distribution and fractionation patterns of POPs in soil; (2) to explain and demonstrate these patterns by using examples drawn from the literature; (3) to quantify the effects of primary and secondary sources on the observed patterns; and (4) to reveal the mechanism of the primary and secondary distributions and fractionations. Given the diverse physical-chemical properties of POPs, the larger number of available datasets in soil than other POPs, and their important role in deriving different fractionation hypotheses, we primarily focus on PCBs in this study. Specifically, we have chosen CB-28 as a representative for low molecular weight PCBs (LMW-PCBs) and CB-180 as a representative for high molecular weight PCBs (HMW-PCBs). Nevertheless, we also discuss a few other POPs within this study.

2. Methods

2.1. Literature review

We searched extensively to include all peer-reviewed papers published after 1993, when Wania and Mackay [41] first introduced the concept of global fractionation. Table S1 provides a comprehensive list of 114 papers that examine the primary and secondary distributions and/or fractionations for different POPs in different matrices. Among these papers, only 26 papers discussed the fractionation issue, with an additional 38 papers focusing on PCBs in the surface soil. The number of the selected papers in Table S1 versus the publishing year is shown in Fig. S2, indicating that 60.5% of these papers were published after 2010 (inclusive).

2.2. P/G partitioning of SVOCs in the atmosphere and major processes between air and soil

As shown in Fig. S3, the four major processes (fluxes) that transfer POPs from air to soil are diffusion (known as a dry gaseous deposition) (F_{AS}), rain and snow scavenging (wet gaseous deposition) (F_{RS} and F_{SS} , respectively) for gaseous POPs, and wet and dry depositions (F_{WD} and F_{DD} , respectively) for particulate POPs. Aerosol particles sorbing POPs exhibit a higher deposition rate than gaseous POPs [41]. The partitioning between gaseous and particulate phases determines the relative portions of POPs in the gas and particle phases, thus controlling all four processes. Thus, the particle/gas (P/G) partitioning of atmospheric POPs is an important and direct influencing factor of POP distribution and fractionation in the soil [42–44]. The P/G partitioning is also important for mountain cold-trapping [45]. Here, we analyzed the P/G partitioning (See details in Text S1.1) and these four processes (See details in Text S1.2) to lay a theoretical ground for the study of the distribution and fractionation patterns of SVOCs in the surface soil.

Notably, previous studies have investigated the role of adsorption in studying P/G partitioning [46–48]. However, the adsorption effect on the P/G partitioning has been found insignificant [49]. Similarly to the P/G partitioning process, absorption into soil organic matter (SOM) is also the dominant partitioning mechanism for the soil/air partitioning process, while adsorption processes can be neglected for most nonpolar SVOCs [50–60]. Thus, this study only considers the absorption process for nonpolar POPs, such as PCBs, organochlorine pesticides (OCPs), and PBDEs.

The steady-state equation (Li-Ma-Yang equation) was developed explicitly to study the P/G partitioning behavior of SVOCs [61]:

$$\log K_{PS} = \log K_{PE} + \log \alpha \quad (1)$$

where K_{PS} is the partitioning quotient at steady state, and K_{PE} is the partitioning coefficient at equilibrium, which is given by Ref. [62]:

$$\log K_{PE} = \log K_{OA} + \log f_{OM} - 11.91 \quad (2)$$

and $\log \alpha$ is given as [61]:

$$\log \alpha = -\log \left(1 + 4.18 \times 10^{-11} f_{OM} K_{OA} \right) \quad (3)$$

where K_{OA} is the octanol-air partitioning coefficient, and f_{OM} is the mass fraction of organic matter in aerosol particles.

The above equations lead to two thresholds for $\log K_{OA}$: $\log K_{OA1} = 11.38$ and $\log K_{OA2} = 12.50$. As shown in Fig. S4, the two thresholds partition the range of $\log K_{OA}$ into *equilibrium* (EQ), *nonequilibrium* (NE), and *maximum partition* (MP) domains, in which the values of $\log K_{PS}$ reach a maximum constant value of $\log K_{PSM} = -1.53$, independent of the values of $\log K_{OA}$ [61]. Notably,

K_{OA} is a strong function of airborne temperature given by equation $\log K_{OA} = A_0 + B_0/T$, where T is the airborne temperature in K, and A_0 and B_0 are given in Table S2 for selected PCB and PBDE congeners. Additionally, we have calculated the temperature thresholds, denoted as t_{TH1} and t_{TH2} , which correspond to the temperatures at which $\log K_{OA}$ of SVOCs reaches the threshold values, $\log K_{OA1}$ and $\log K_{OA2}$. For CB-28, t_{TH1} is calculated as -34.0 °C, and t_{TH2} as -48.1 °C. For CB-180, the values are $t_{TH1} = 8.5$ °C and $t_{TH2} = -9.5$ °C (Fig. S5).

The logarithm of K_{PS} values for CB-28 and CB-180, together with their ratios, as a function of temperature from 30 to -30 °C, is presented in Fig. S6. The results indicate that, at the same temperature, $\log K_{PS-180}$ is higher than $\log K_{PS-28}$. The ratio of K_{PS-180}/K_{PS-28} decreases as the temperature decreases, from 340 at $t = 30$ °C to 2.8 at $t = -30$ °C. These findings suggest that, at the same temperature, the particle fractions of CB-180 are higher than those for CB-28, and their ratios decrease as the temperature decreases. Fig. S7 depicts ϕ_p for CB-28 and CB-180, as well as their ratio, in relation to temperature, assuming $TSP = 50 \mu\text{g m}^{-3}$. The results reveal that the particle fractions of CB-180 are higher throughout the entire temperature range than those for CB-28. Specifically, within the temperature range of 30 °C to -30 °C, the particle fractions for CB-28 were from 0.03% to 34.07%, whereas CB-180 ranged from 9.41% to 59.48%. Furthermore, their ratios decrease with decreasing temperature, from 304 at $t = 30$ °C to 1.75 at $t = -30$ °C. This suggests that in scenarios where equal amounts of CB-180 and CB-28 are introduced into the atmosphere devoid of these compounds, significantly larger quantities of CB-180 than CB-28 will be sorbed onto aerosol to reach the steady state.

POPs in the surface soil may go back to air through volatilization to compensate for the flux from air to soil (F_{AS}). The net flux between air and soil depends on the fugacity of the gaseous POPs in the air (f_G) and soil (f_S). At the initial stage, $f_G > f_S$, the soil acts as a *sink*, resulting in a net flux of POPs from air to soil. When POPs reach an equilibrium between air and soil, or when $f_G = f_S$, the net flux equals zero. Conversely, when $f_S > f_G$, there is a net flux of POPs from soil to air, and the soil acts as a secondary source. Therefore, this relationship between f_G and f_S is important, as it determines the strength of the respective sources: the primary source prevailing when $f_G > f_S$, or the secondary source when $f_G < f_S$. If the airborne temperature is below zero and the soil is covered by snow, the flux from air to soil should be replaced by that from air to snow (F_{ASn}), which is discussed in Text S1.2.

When POPs reach equilibrium between air and soil, the ratio of its concentration in soil to its gaseous concentration in air is given by $C_S/C_G = K_{SA}$, where K_{SA} is the soil–air partitioning coefficient, given by $K_{SA} \approx f_{SOM} K_{OA}$ when temperature is above zero. This relationship indicates that K_{SA} is proportional to K_{OA} and soil organic matter content (f_{SOM}) and increases at colder temperatures, aligning with K_{OA} . As shown in Fig. S8, at the same temperature, the values of K_{SA} for CB-180 are higher than CB-28 by ~ 3 orders of magnitude. When the temperature drops from 30 to 0 °C, the values of K_{SA} increase by ~ 1.5 orders of magnitude for CB-28 and ~ 1.8 orders of magnitude for CB-180. A global gridded map of $\log K_{SA}$ values was produced for CB-28 and CB-180 [39]. The map clearly illustrated that CB-180 exhibited higher K_{SA} values than CB-28 at identical locations. Furthermore, K_{SA} increased along with decreased temperatures from the equator towards the poles, applicable to CB-180 and CB-28. A higher K_{SA} value for a particular chemical indicates stronger retention by the soil. Thus, CB-180 exhibits a greater retention capacity in the soil than CB-28. Furthermore, this retaining ability increases along with the decrease of the ambient temperature. Therefore, the re-entry of CB-180 from the soil back into the air is considerably more challenging

than that of CB-28. Alternatively, the switch of soil from a sink to a source will take much longer for CB-180 than for CB-28.

Detailed equations related to the processes between air and soil can be found in **Text S1.2**. The fluxes for these major processes between air and soil for CB-28 and CB-180 calculated from these equations are presented in **Fig. 1**. The fluxes for the individual processes are shown in **Fig. S9**. To facilitate comparison, we assume the total air concentration (gas phase + particle phase) of 100 ng m^{-3} for both CB-28 (0.39 mol m^{-3}) and CB-180 (0.25 mol m^{-3}). For CB-28, with lower K_{OA} values, total fluxes from air to soil are dominated by the diffusion of gaseous CB-28, except when the temperature falls below $-21 \text{ }^\circ\text{C}$ (**Fig. 1**). At temperatures below this threshold, particle deposition emerges as the primary contributor to the flux from air to soil. Notably, this air-to-soil flux is compensated to a certain extent by the volatilization of CB-28 from soil to air. In contrast, for CB-180, which has higher K_{OA} values, particle deposition is always the major factor determining the flux from air to soil over the entire range of temperatures from 30 to $-30 \text{ }^\circ\text{C}$. At any ambient air temperature, CB-28 and CB-180 significantly transfer from air to soil at the source region. However, as these compounds disperse from the source, the magnitude of their transfers decreases, establishing the primary distribution pattern for each compound. The higher total fluxes from air to soil for CB-180 than CB-28, plus the stronger potential of soil to retain CB-180 than CB-28, contributes to the primary fractionation for these two chemicals: an enrichment of CB-28 and a depletion of CB-180 with increasing distance. The primary distribution and fractionation patterns are primarily determined by the distance or remoteness from the source in all directions rather than being primarily influenced by the air temperature. As depicted in **Fig. 1**, a trend of generally increasing flux can be observed as the temperature decreases for CB-180 and CB-28. For CB-180, the fastest increasing trend (approximately by a factor of 7) occurs when $t \geq 0 \text{ }^\circ\text{C}$, increasing from $8.47 \times 10^{-7} \text{ mol h}^{-1}$ at $t = 30 \text{ }^\circ\text{C}$ to $4.31 \times 10^{-6} \text{ mol h}^{-1}$ at $t = 0 \text{ }^\circ\text{C}$, and then almost remains constant ($\sim 6.10 \times 10^{-6} \text{ mol h}^{-1}$) when $t \leq 0 \text{ }^\circ\text{C}$. For CB-28, the total flux increases from $1.84 \times 10^{-7} \text{ mol h}^{-1}$ at $t = 30 \text{ }^\circ\text{C}$ to $3.69 \times 10^{-7} \text{ mol h}^{-1}$ at $t = 0 \text{ }^\circ\text{C}$ and from $2.14 \times 10^{-6} \text{ mol h}^{-1}$ at

$t = 0 \text{ }^\circ\text{C}$ to $5.39 \times 10^{-6} \text{ mol h}^{-1}$ at $t = -30 \text{ }^\circ\text{C}$, demonstrating a substantial factor of 29 increase. The fast increase in CB-28 fluxes provides the main mechanism that forms the secondary distribution pattern for this compound. It is worth mentioning that the secondary distribution pattern depends strongly on airborne temperature, making it most discernible along transits exhibiting a pronounced airborne temperature gradient, frequently aligned in latitudinal or altitudinal direction.

As discussed above, P/G partitioning and the four processes are all related to K_{OA} . Therefore, the parameter K_{OA} plays a critical role in all processes responsible for transferring POPs from air to soil and determining the net flux of air–soil exchange. The difference in the removal efficiency of CB-28 and CB-180 from air to soil is mainly due to the contrast in K_{OA} at any given temperature, which will vary with air temperature. Since K_{OA} is a strong function of air temperature, air temperature is a critical factor in determining P/G partitioning and the relative importance of each process. This is important when trying to understand the distribution and fractionation patterns of POPs, which will be explored later. Two factors may lead to the observed distribution and fractionation patterns of POPs in the soil: one is the primary factors or the physicochemical properties (K_{OA} , for example) and the distance from the source; and the second factor is airborne temperature, displaying clearly along latitude transect.

As introduced earlier, the secondary distribution and fractionation patterns can also occur altitudinally; however, the mechanism from the secondary factors along altitude is more complicated. Thus, we firstly focus on the secondary phenomena along the latitudinal transect and subsequently delve into discussing phenomena along the altitudinal transect in **Section 5**.

It is worth noting that the subcooled liquid vapor pressure (P_L) has also been used for calculating the P/G partitioning quotient [48,63,64]. Yang and co-workers [65] have reported that the parameters P_L and K_{OA} can be linked by a simple equation: $\log K_{OA} = -\log P_L + 6.46$. Using this relationship, any equation based on K_{OA} can be transferred to one based on P_L , and vice versa. However, the parameter K_{OA} has been predominantly favored in modeling the transport and fate of POPs, since octanol is a suitable surrogate of organic matter in soil, aerosol particles, and other matrices containing organic matter. In contrast, the parameter P_L lacks this advantageous characteristic.

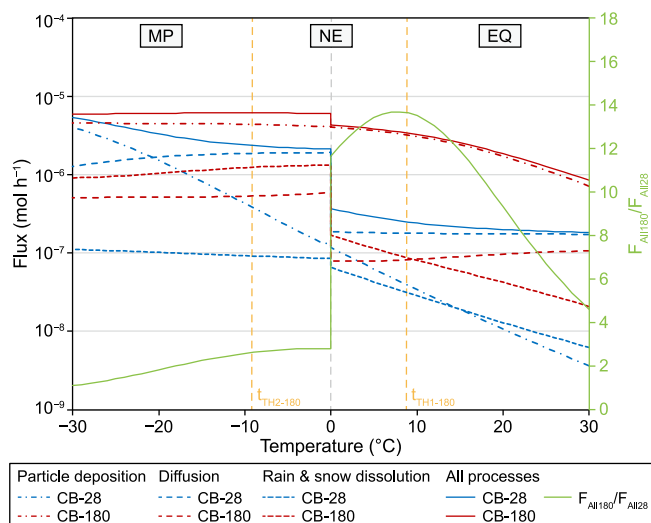


Fig. 1. Fluxes for the major processes (particle deposition, gaseous diffusion, and rain and snow scavenging) for CB-28 and CB-180 as a function of temperature from -30 to $30 \text{ }^\circ\text{C}$. The two vertical dashed yellow lines are the temperature thresholds for CB-180, which divide the temperature into three domains (ER, NE, and MP domains) for CB-180 (Assuming $TSP = 50 \text{ } \mu\text{g m}^{-3}$, $C_A + C_P = 100 \text{ pg m}^{-3}$, which are concentrations of CB-28 or CB-180 in the gas phase and particle phase).

2.3. Quantification of primary and secondary source effects

To study the influences of human activities and environmental factors on the spatial distribution of PBDEs in the surface soil, Li and co-workers [31] developed a multiple linear regression equation. They considered three independent variables: temperature in the sampling site (T , in K), soil organic carbon (f_{SOC} , in %), and area population density (PD , the surrogate of the primary area source). Later, the fourth variable, the distances from the sources (D_i), was added by the equation [32], and a multiple linear regression equation with the four independent variables was obtained. In this study, we have employed two modified forms of the equation to analyze the data, as follows:

$$\ln C_S = a \ln S_A + \sum b_i \ln D_i + cT + df_{SOM} + e \quad (4)$$

using natural logarithms or base ten logarithms as

$$\log C_S = a \log S_A + \sum b_i \log D_i + cT + df_{SOM} + e \quad (5)$$

where C_S is the concentration of an SVOC in the soil, S_A is an area source (usually using a surrogate, such as population density, PD),

D_i the distance from the point source i , f_{SOM} the soil organic matter content (%), and a , b_i , c , d , and e are normalized regression coefficients.

In this study, we define the first two terms, a and b_i , as the primary terms, followed by the two secondary terms, c , and d . The final term, e , is related to the background concentration of the chemical. To assess the dominant factors influencing the distribution, we compare the magnitudes of these terms. If $|a| + |\sum b_i/n| > |c| + |d|$, the primary factors play a major role, indicating a primary distribution. Conversely, if $|c| + |d| > |a| + |\sum b_i/n|$, the secondary factors dominate, resulting in a predominantly secondary distribution. When $|a| + |\sum b_i/n| = |c| + |d|$, the chemicals are in the transiting phase, switching between the primary and secondary distributions. This method serves as the criterion to distinguish the relative importance of primary and secondary factors. The half distance ($D_{1/2}$) represents the distance where the chemical concentration decreases by half of the value at the point source. This parameter facilitates the comparison of the travel abilities among chemicals. These equations are especially useful when an area source of a POP is under consideration.

3. Primary and secondary distribution patterns

3.1. Primary distribution patterns of POPs in the soil

3.1.1. Point source and point pulse

If a single point source can be identified, the influence of that source on POP distribution, showing a “point pulse”, could be easily identified. By considering the second and last term in equation (4), we obtain the following relationship between concentration and distance [66]:

$$\ln C_S = b \ln D + e \quad (6)$$

where C_S is the concentration in the soil at a distance of D (km) from the source center, b is the slope, and e is the natural logarithm of the background concentration of the chemical.

Li et al. measured concentrations of BFRs, including PBDEs, in the surface soil surrounding two chemical plants manufacturing BFRs in China [24]. A linear relationship between the natural logarithm concentration of BDE-209 in the soil and the natural logarithm distance from the source center was found for both two plants. Two linear equations were found to represent BDE-209 concentrations in the soil around the two manufacturers:

$$\ln C_S = -1.149 \ln D + 15.838 \quad (7)$$

for Plant 1 (Fig. 2) and similarly

$$\ln C_S = -1.426 \ln D + 17.851 \quad (8)$$

for Plant 2. Based on the equations, it can be observed that Plant 1 exhibits a $D_{1/2}$ at 0.365 km, whereas Plant 2 demonstrates a slightly larger value of $D_{1/2}$ at 0.370 km. These results indicate a decreasing trend with the distance increases, with both plants having nearly identical values of $D_{1/2}$ for the pulse shape under consideration.

Wang et al. reported a similar finding for dechloranes in the soil surrounding a DP manufactory in China [20]. These authors determined that DP concentrations in the soil (C_S) from DP manufacturing plant could be expressed as a function of distance (D):

$$\log C_S = -1.14 \log D + 1.97 \quad (9)$$

Primary distribution patterns associated with point sources

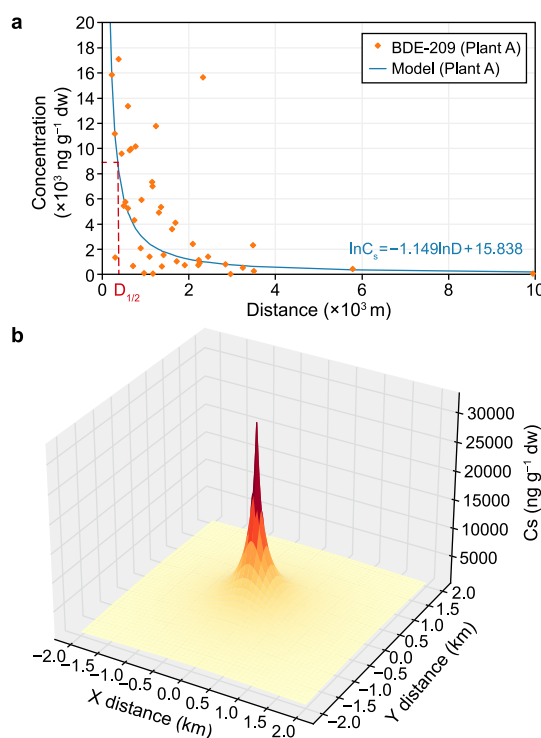


Fig. 2. BDE-209 concentrations in the soil from a BFR manufacturing plant as a function of distance, showing pulse distribution patterns. a, One-dimensional graph. b, Three-dimensional graph. Data are taken from Li et al. [24].

have also been reported for PBDE and TBBPA concentrations in the surface soil around an e-waste site in Longtang, China [23], and Σ PBDEs and Σ NBFRs concentrations in the surface soil surrounding two e-waste recycling facilities in Australia [26]. These two studies revealed a strong negative correlation between chemical concentrations and distance from the sources.

Another good example of a point-source primary distribution pattern has been provided by historical and emerging flame retardant concentrations in Chinese forest soils [67]. It reveals that the concentration distributions in the soil were primarily controlled by the distribution of industrial sources, including fire retardant manufacturing plants within the region.

3.1.2. Urban source and urban pulse

The distributions of PCBs originating from urban sources have been extensively studied in various locations worldwide. For instance, research conducted in Toronto, Canada, examined the distribution of PCBs in the air [15]. In another study, the distribution of PCBs in the soil was investigated along a transect in Shanghai, China [28]. Similarly, the distribution of PBDEs in the soil was analyzed along a rural-urban-rural transect in Kuwait [68]. In Stockholm, Sweden, a comprehensive study investigated the distribution of HMW PBDEs in the soil and several flame retardants in the air along a transect [17]. Moreover, the distribution of PBDEs in the air around Birmingham, the UK, was also examined [56]. This kind of primary distribution pattern was also called the “urban pulse” [17,56], which indicates the source as an urban and the primary distribution pattern as a pulse. A generalized urban source involving several urban centers was also observed. The urban centers exhibited the highest total PCB concentrations, followed by those in rural sites, and the background sites on Chinese soil with the lowest concentrations [28]. The overall concentrations of PBDEs followed the order of urban > rural > background sites in Chinese

air [69] and in the soil across five Asian countries, i.e., China, India, Japan, South Korea, and Vietnam [31].

3.1.3. Area sources

In certain cases, the origins of target pollutants do not stem from a specific localized point or an urban center, but rather from a broader region that can be symbolized by a surrogate indicator like population density. Here, we might use the PD in equation (4) to represent the S_A as follows:

$$\ln C_S = a \ln PD + e \quad (10)$$

Li and co-workers (2017) reported residues of 19 NBRFRs in the soil of five Asian countries, i.e., China, India, Japan, South Korea, and Vietnam [32]. The results showed a significant positive correlation between the natural logarithm of concentrations and the natural logarithm of PD . Similar correlations between concentration and PD were also observed for PBDEs in the surface soil in the five Asian countries [32]. Zhang et al. [70] reported PCB and PBDE concentration distributions in the soil across Scotland. They found that PCBs and PBDEs were higher in the two southern transects than in the two northern transects. This may be due to the proximity to areas of high population and industrial activity in the south. These results revealed a primary distribution pattern with area sources.

The usages of OCPs are also considered as area sources. Previous studies have also examined the primary distribution patterns of OCPs associated with area sources. For example, endosulfan concentration in Chinese agricultural surface soils has been found to follow a primary distributing pattern similar to the usage pattern of this pesticide [71].

3.1.4. Longitudinal primary distribution

Longitudinal primary distribution was first observed for PCBs [28] and followed by PBDEs [31] in Chinese surface soils. As shown in Fig. 3c, a significant correlation (with $R^2 = 0.23$, $p = 0.003$) has been found between the logarithm of Σ PCBs concentrations in Chinese rural/background soil and the corresponding longitude from 94° to 122° E (~ 3000 km).

Although longitudinal distribution for PCBs does not directly point to a primary source, this distribution pattern does follow the general characteristics for a primary distribution pattern, consistent with their usage pattern in China, decreasing from east to west

(Fig. 3a), whereas the concentrations of PCBs is strongly correlated with their usage data per grid cell with $R^2 = 0.32$ and $p < 0.001$ [72], as shown in Fig. 3b. The relationship between concentration C_{PCB} and the PCB usage U_{PCB} can be expressed as follows:

$$C_{PCB} = 0.3545U_{PCB} + 179.38 \quad (11)$$

This longitudinal distribution pattern may be observed only in China due to a unique PCB and PBDE (or other industrial pollutants) usage pattern in this country, as depicted in Fig. 3a, revealing that the PCB usage per grid cell in Chinese soil are strongly linked with longitude from 74° to 120° E with $R^2 = 0.71$ and $p < 0.001$, decreasing from east to west in China [72].

3.1.5. Latitudinal primary distribution

Latitudinal primary distribution has been reported by Meijer et al. [27] for PCBs in background soil in the UK and Norway from 50° to 75° N. Here, we consider the Norwegian data only from 58.3° to 75° N, and the reason is discussed in Section 7.4. This decreasing trend for PCB concentrations in Norwegian soil was evident, as presented in Fig. 3g, showing a strong and significant correlation between PCB concentrations and latitude in Norway with $R^2 = 0.31$ and $p = 0.001$. The primary nature of this latitudinal decreasing pattern can be identified from Fig. 3f, indicating that PCB concentrations in Norwegian soil were strongly linked with PCB usage ($R^2 = 0.58$ and $p = 0.007$). This finding aligns with the strong and significant correlation observed in Chinese rural and background soil, as discussed in the previous subsection. The source is also an area one, and the relationship between concentration (C_{PCB}) and usage (U_{PCB}) can be expressed as follow:

$$C_{PCB} = 1.0306U_{PCB} + 821.6 \quad (12)$$

This is attributed to the decreasing trend of PCB usage from south to north in Norway, similar to that from east to west in China (described in the previous subsection). Importantly, a strong and significant correlation ($R^2 = 0.45$ and $p = 0.008$) exists between PCB usage and latitude from south to north in Norway, as shown in Fig. 3e. The strong and significant correlations between PCB concentrations and their usage (Fig. 3f) and between the usage and latitude (Fig. 3e) lead to the correlation between PCB concentration and latitude (Fig. 3g). The leading factor is the decreasing trend of PCB usage from south to north along latitude in Norway, which

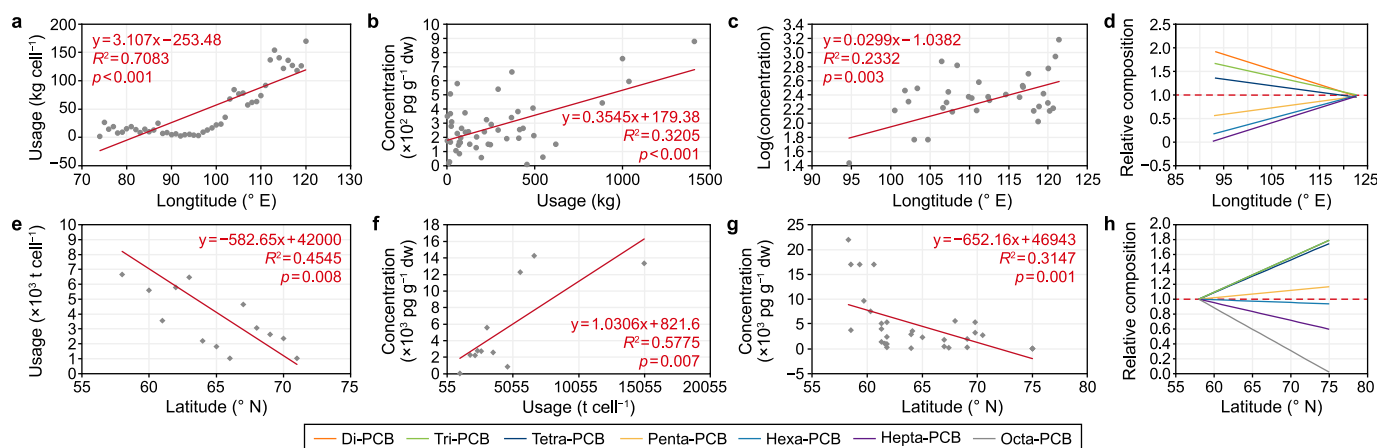


Fig. 3. a–d, Longitudinal distributions and fractionations based on data from China. a, PCB usage versus longitude. b, PCB concentration versus PCB usage. c, PCB concentration versus longitude. d, Relative compositions of PCBs versus longitude. e–h, Latitudinal distributions and fractionations based on data from Norway. e, PCB usage versus latitude. f, PCB concentration versus PCB usage. g, PCB concentration versus latitude. h, Relative compositions of PCBs versus latitude. Note: PCB concentration data in Chinese soil are taken from Ren et al. [28]; PCB concentration data in Norwegian soil are taken from Meijer et al. [27]; PCB usage data in China are taken from Zhang et al. [72]; and PCB usage data in Norway are taken from Breivik et al. [3,4].

aligns with the primary distribution.

The striking similarities for PCBs in the soil between the longitudinal distribution in China from east to west and the latitudinal distribution in Norway from south to north are observed (Fig. 3). Despite the existence of a temperature gradient along the latitudinal transect in Norway, it appears that temperature variations may not have a significant impact on shaping the latitudinal distribution pattern of PCBs in Norwegian soil.

3.2. Secondary distribution pattern of POPs in the soil

The secondary distribution pattern of PCBs in the soil has been reported by Wang and co-workers [73]. Forty background surface soil samples were measured in the Qingzang Plateau, China. A positive, strong, and significant correlation ($R^2 = 0.96$, $p = 0.008$) was found for tetra-PCBs along the latitude from 28.2° to 37.1° N, showing a secondary distribution pattern.

Secondary distribution patterns have also been reported for other POPs by different groups. For example, this pattern was clearly observed for α -HCH in Chinese soils. Technical HCH was historically applied in far greater quantities in southern China, but high concentrations of α -HCH, a leading component of technical HCH, were found in the soil from northeast China [40,74]. This was illustrated by plotting the usages and soil concentrations at five sites from southmost Site 1 (30.1° N) to northmost Site 5 (51.5° N) (Fig. 4). The total usage of α -HCH was ~ 1000 kg m^{-2} at Site 1, decreasing to ~ 5 kg m^{-2} at Site 5. The concentration of α -HCH measured from June 2005 to June 2006 was ~ 2 ng g^{-1} dw at Site 1, and increased by one order of magnitude to ~ 12 ng g^{-1} dw at Site 5, showing a clear secondary distribution pattern [40].

4. Primary and secondary fractionation patterns

4.1. Primary fractionation pattern

4.1.1. Point source fractionation

Point source fractionation was first identified in the soil near BFR-related industrial sites in China [24]. The HMW NBFs and PBDEs were deposited to soils closer to the industrial and e-waste sites, while the LMW NBFs and PBDEs were deposited far away from the sites. This fractionation was also found for BFRs in the surface soil surrounding two e-waste recycling facilities in Australia [26].

4.1.2. Urban fractionation

Urban fractionation in the soil is demonstrated in Fig. 5,

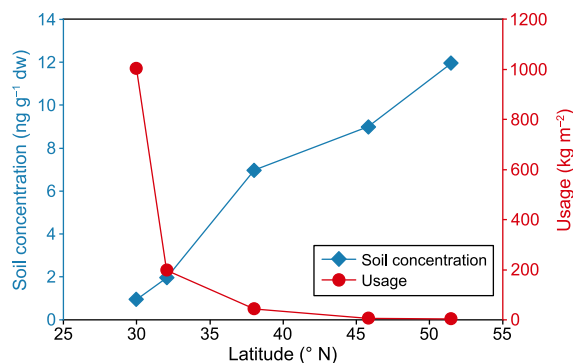


Fig. 4. The total usages and measured soil concentrations of α -HCH in 2005–2006 at five sites from the south (30.1° N) to the north (51.5° N) of China. Data are taken from Liu et al. [40].

showcasing the distribution of six PCB homologs (di-, tri-, tetra-, penta-, hexa-, and hepta-PCBs) in Shanghai and its surrounding area, China [28]. Site U0 was located within the city, and Sites R1, R2, and R3 were ~ 100 , ~ 400 , and ~ 500 km to the west of the city, respectively. The total concentration of PCBs at the four sites correlated with the distances away from the city with $R^2 = 0.88$ and $p = 0.06$. Over this urban-rural transect, the relative concentrations for these six homologs observed in monitoring data correlated with distances from the central urban site. The observed trend showed an enrichment of the LMW di- and tri-PCBs and a depletion of the hexa- and hepta-PCBs with increasing distance from the urban center. However, the relative concentrations for tetra- and penta-PCBs remained almost unchanged. Furthermore, a broader urban fractionation phenomenon involving several urban centers was also observed. At the national scale of China, surface soils from urban sites in China displayed relatively higher proportions of HMW PCBs, whereas soils from rural sites exhibited higher levels of LMW PCBs, thus providing strong evidence of large-scale urban fractionation [75].

Urban fractionation has been found in various regions. For instance, in the Pearl River Delta, LMW PCBs were the major congeners detected in distal areas lightly impacted by industrial activities, while HMW PCBs were more prevalent near industrial centers like Shenzhen, Zhongshan, and Guangzhou, China [76]. Similarly, in Manipur, India, relatively high concentrations of HMW PCBs homologs were found near local sources, contrasted with the increased relative contribution of LMW PCBs to distant soils [77]. In Europe, LMW PCBs tend to be in equilibrium with the f_{SOM} , while HMW PCBs tend to be confined close to the source areas [29].

4.1.3. Longitudinal fractionation

As pointed out in Section 3.1.4, longitudinal primary distribution was observed for individual PCB and PBDE congeners in Chinese soils, which also displayed longitudinal fractionation patterns for PCBs [28] and PBDEs [31]. This pattern follows the general characteristics of a primary distribution pattern, given that PCBs in Chinese soil decrease from east to west. As displayed in Fig. 3d, the relative composition of homolog groups, normalized to the percent composition for the longitude band of 120 – 125° E, where all values are unity, indicates the effect of fractionation on PCBs as they westward transport. Specially, LMW PCB homologs (di-, tri-, and tetra-PCBs) became enriched, while HMW PCB homologs (penta-, hexa-, and hepta-PCBs) became depleted. This is a typical primary longitudinal fractionation pattern.

4.1.4. Latitudinal fractionation

The first reported latitudinal fractionation in the soil was obtained with the PCBs in background soil in the UK and Norway from 50° to 75° N [27]. The percent composition of the PCB profile was determined for each site and normalized to the percent composition for each homolog (tri-, tetra-, penta-, hexa-, hepta-, and octa-PCBs) at the southmost site in Norway, where all the relative concentrations are unity (Fig. 3h). The relative concentrations of LMW PCBs (e.g., tri- and tetra-PCBs) increased with latitude, while those of HMW PCBs (e.g., hepta- and octa-PCBs) decreased. The penta- and hexa-PCBs have almost equal relative concentrations of these homolog groups. This was considered consistent with the global fractionation theory, showing a preferential transport of more volatile compounds to higher latitudes.

4.2. Secondary fractionation pattern

Wang and co-workers [73] reported the discovery of tetra-PCB evidence showcasing a correlation with latitude ($R^2 = 0.96$, $p = 0.008$) and a slight positive slope of 0.057, thereby suggesting

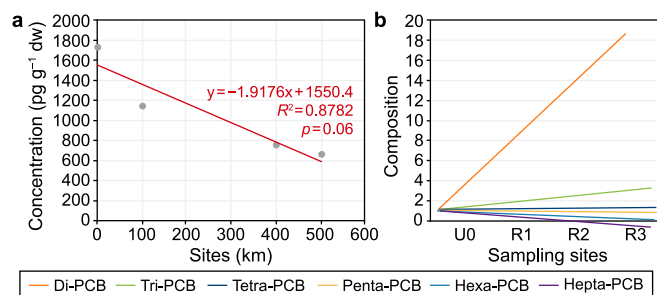


Fig. 5. The relative composition of PCB homologs in soil samples at sites U0, R1, R2, and R3. All the values were normalized to the percent composition for Site U0, where all values are unity. Data are taken from Ren et al. [28].

latitudinal fractionation in the surface soil in the Qingzang Plateau, China. However, this interpretation is flawed as it confuses a secondary distribution pattern (See Section 3.2) with fractionation, which cannot be observed for a single PCB homolog. The real evidence of the secondary fractionation can be obtained by analyzing the data for two PCB congeners, CB-28 and CB-52, from the same study by Wang et al. [73]. Analysis of variation in CB-28 and CB-52 along with the latitude, as presented in Fig. 6, revealed that CB-28 levels increased along the latitude ($R^2 = 0.17$, $p = 0.01$), showing a secondary distribution pattern. Conversely, CB-52 levels decreased along the latitude ($R^2 = 0.12$, $p = 0.07$), showing a primary distribution pattern. The combined behavior of these two congeners displayed a secondary latitudinal fractionation pattern, which could represent the first reported evidence for such fractionation for PCBs in surface soils. However, this still be debatable, as discussed in Section 7.4.

Secondary fractionation of PCBs on global lowland soil has not yet been identified, most likely because fresh PCBs escape from e-waste sites, old equipment, and old buildings containing PCBs. Furthermore, the emission of unintentional-produced PCBs (UP-PCBs) as byproducts of industrial processes has become the major source of PCBs in some countries, possibly maintaining a primary distribution pattern in the soil [78].

5. Altitudinal distributions and fractionation of POPs

While the secondary distribution pattern and the secondary fractionation have been hardly observed on lowlands, they have been frequently reported along the slopes of mountains. Blais and co-workers published the first report on the altitudinal accumulation of POPs in mountainous areas [79]. This study measured PCBs and OCPs in the snow in Western Canadian mountains. Their

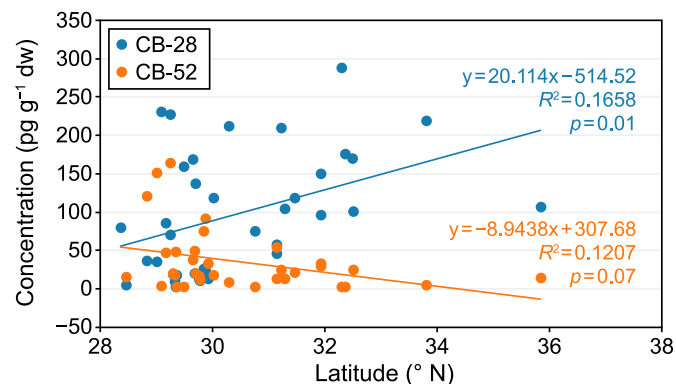


Fig. 6. Latitude distribution of CB-28 and CB-52, showing a secondary fractionation pattern. Data are taken from Wang et al. [73].

results showed the secondary distribution pattern for LMW di- and tri-CB congeners and the primary distribution pattern for HMW hepta-CBs. Consequently, these results elucidated a secondary fractionation pattern among these compounds (Fig. S10).

Numerous studies have been carried out following the work by Blais and co-workers, such as studies in the surface soil for PAHs [80], PCBs and OCPs [81], PCBs and selected OCPs [82,83], PCBs and PBDEs [84–86], and OCPs in the soil [55,73,87–89]. Five studies investigated PCBs in surface soils within the Qingzang Plateau, China [82,84–86,90]. In addition to the aforementioned findings, several studies have investigated the presence of various pollutants in different media. For example, one study focused on PCBs, PAHs, and selected OCPs in snow cores [91]. Another study examined PCBs, OCPs, and additional selected organochlorine compounds (OCs) in lake fish and sediment [92], as well as mosses [93]. Additionally, investigations have analyzed the levels of OCPs in both the air, with a specific focus on lichen [55] and air and spruce needles [87]. Furthermore, a study investigated the presence of PCBs and PBDEs in lake fish [94].

A so-called “mountain cold-trapping” has been used to explain the observed altitudinal concentration gradients of POPs [92]. On the one hand, mountain cold-trapping is similar to polar cold-trapping, in which POPs are transported to higher altitudes via multi-hoppers or repeated cycles of deposition and evaporation. Chen et al. [82] investigated the soil in Balang Mountain, China, collected in the autumn of 2006, and identified the presence of CB-28 and CB-52. Their findings revealed a higher trapping efficiency for the lighter CB-28 than the heavier CB-52, with a secondary distribution pattern for each congener and a combined secondary fractionation pattern for both congeners (Fig. S11). The levels and compositions for PCBs in the soil in Italian Alps were determined by Tremolada and co-workers [83], showing that the LMW PCBs increased along the slope of the mountain, while the HMW PCBs showed a decreasing trend. These examples confirmed the tendency of the less chlorinated congeners to be preferentially transported at high altitudes, which is the same as those for polar cold-trapping, enrichment for LMW PCBs, and depletion for HMW PCBs in background soil from southern UK to northern Norway [27]. Consequently, similar secondary fractionation patterns are observed among these compounds. On the other hand, these two trapping mechanisms are different, as extensively discussed by Wania and Westgate [45,95]. They suggested that the wet deposition due to temperature-induced precipitation is the key factor distinguishing mountain cold-trapping and polar cold-trapping, thus influencing altitudinal and latitudinal fractionations. They also predicted that heavier PCBs, rather than lighter ones, will preferentially concentrate upslope on a mountain, aligning with reported observations [82,84,90,92,94,96].

Complicated phenomena regarding PCBs in the soil have been observed and documented. Wang et al. [84] have identified two opposite trends of log-transformed total organic carbon (TOC)-normalized concentrations of PCBs and PBDEs in the surface soil from the Qingzang Plateau, China. A negative relationship was observed below an altitude of approximately 4500 m, followed by a positive altitude dependence above this threshold. Zheng and co-workers [85] measured the concentrations of PCBs and PBDEs in Balang Mountain, China. They found that the TOC-normalized concentrations of these contaminants were higher in samples from the lower mountain, below the treeline, than those from the upper mountain with alpine meadow. The forest filter effect was identified as a potential explanation for this variation. In another study, Meng and co-workers [86] studied the altitudinal distribution of PCBs and PBDEs in the surface soil samples collected along two sides of Mt. Sygera, southeast of the Qingzang Plateau. Surprisingly, the relationships between concentrations of the two

groups of POPs and the altitudes showed different trends on the windward and leeward sides. The windward side exhibited positive and significant correlations for heavier PCB congeners (e.g., CB-138 and CB-180), whereas lighter PCB congeners (e.g., CB-28 and CB-52) showed negative and significant correlations (Fig. S12a), forming a nice secondary fractionation pattern (Fig. S12b). However, on the leeward side, all PCB congeners (e.g., CB-28, CB-52, CB-138, and CB-180) displayed a negative correlation with altitude above 4100 m, which was different from the increasing trends of these congeners below 4100 m, as shown in Fig. S13a, and did not display a fractionation pattern (Fig. S13b).

According to the discussions above, we suggest that these differences are caused by the local conditions, such as local climate and vegetation condition, and soil contents. However, the underlying mechanisms for generating these different results have not been comprehensively investigated. Consequently, further studies are needed to reveal these different distribution and fractionation patterns for POPs along altitude transect in remote mountains. Similar suggestions were also brought up by Shen et al. [87] and Meng et al. [86].

6. Modeling primary and secondary distribution patterns and fractionation effects

Only a few studies have investigated the distribution and fractionation patterns based on modeling [12,42,97–103]. Wania and Su [12] applied a zonally averaged global fate and transport model (Globo-POP) to simulate the compositional shifts of PCBs as a function of the environmental compartment, latitude, and time. Model results indicated that relative abundance increased for lighter PCB congeners whereas decreased for heavier ones with increasing latitude, which had been observed in field studies and agreed with the global fractionation hypothesis. Using a simple conceptual model (CliMoChem), Scheringer [42] was able to simulate the primary fractionation for three PCB congeners (CB-28, CB-101, and CB-180), and the results were in good agreement with the field data measured by Meijer et al. [27] in European soils.

Similar research was carried out by Stemmler and Lammel [102], who used a multi-compartment chemical-transport model (MPI-MCTM) [104,105] to study the fractionation, transport, and fate of four PCB congeners (CB-28, CB-101, CB-153, and CB-180) from 1950 to 2010. The model predictions indicated that trends of declines of PCB levels along with their compositions in soil would not only be observed along latitudinal lines, but also along longitudinal gradients, which was confirmed by the study by Ren et al. [28] and Li et al. [31]. The authors also found that, in 2010, on the Eurasian Continent, the maximum zonally averaged soil and vegetation burden for CB-180 was still located in the GSR, showing a primary distribution pattern, while the maxima portion for other three congeners located further north. Interestingly, only CB-28 has the maximum burden located $>70^\circ$ N with a second maximum $<60^\circ$ N, showing a secondary distribution pattern. Therefore, these four PCBs form a secondary fractionation pattern.

To investigate the environmental behavior, and the distribution and fractionation patterns of POPs, Cui and co-workers developed a Chinese Gridded Industrial Pollutants Emission and Residue Model (ChnGIPERM). This model was used to explore the distribution patterns and fractionation phenomena for four PCB compounds, including CB-28, CB-101, CB-153, and CB-180 [98]. A single-source site located in eastern central China ($118^\circ 22' - 119^\circ 14' E$; $31^\circ 14' - 32^\circ 37' N$) was assumed with an emission rate of 1 kg d^{-1} from a source (S1) for 1965 only, and the potential for long-range atmospheric transport (LRAT) and fractionation were simulated for 45 years, spanning from 1965 to 2010. Fig. S14 presents an intriguing finding regarding the temporal variation of the relative

concentration of CB-28 at the three northward sites (F1, F2, and F3) in the order from the closest to Site F1 over five time periods, 1966–1970, 1970–1980, 1980–1990, 1990–2000, and 2000–2010, after emissions stopped in 1966 [98]. Assuming the concentrations at F1 in the five periods were all equal to 1, the concentrations of CB-28 decreased along with the distances from F1 to F3 in the first two periods (1966–1970 and 1970–1980), showing a primary distribution pattern. However, the concentrations increased during the last two periods (1990–2000 and 2000–2010), indicating a secondary distribution pattern. The distribution in 1980–1990 was quite even, identifying the critical time when the CB-28 distribution in the soil shifted from the primary to secondary distribution pattern. The secondary distribution pattern in the last two periods (1990–2000 and 2000–2010) can form a secondary fractionation with the other three congeners.

This study presents the development of a one-dimensional and conceptual fugacity model, referred to as the 1D-POP-AS model, to investigate the transport and transfer of POPs between air and surface soil. The model utilizes the equations listed in Text S1 to simulate the transport of CB-28 and CB-180, and the formation of their longitudinal and latitudinal distributions and fractionations. Two compartments, namely air and surface soil, are considered in this model, with both the gas and particle phases taken into account in the air compartment. The results of the model are shown in an animation video titled “Animation_PCB28&180.gif” in SI, which simulates conceptively and animatedly the spatial concentration distributions of CB-28 and CB-180 in the air and soil in continuous time series, showing the transport of these two chemicals. The above two panels in the animation present the transport of CB-28 and CB-180 in 365 days in the air (the top left panel) and in the soil (the top right panel) from the start of their emissions. The results indicate that both CB-28 and CB-180 can undergo LRAT. Notably, CB-28 exhibits a higher transport potential compared to CB-180. Each chemical shows a primary distribution pattern, while together they exhibit a primary fractionation pattern after a certain distance from the source. The middle two panels depict the transport of CB-28 and CB-180 in the air (the middle-left panel) and in the soil (the middle-right panel) over 80 years after the cessation of their emissions, without considering temperature variations. The findings suggest that neither CB-28 nor CB-180 form the secondary distribution pattern. Consequently, both chemicals exhibit the primary fractionation pattern rather than the secondary one. This simulates the longitudinal transport of these two chemicals. The bottom two panels depict the transport of these two chemicals in the air (the bottom left panel) and soil (the bottom right panel) over 80 years along a latitudinal direction after the cessation of their emissions. It indicates that CB-28 can form the secondary distribution pattern and display a secondary fractionation with CB-180 along a latitudinal transect with a decreasing temperature gradient in the air and soil after ~40 years. In contrast, CB-180 fails to form the secondary distribution pattern in air or soil, even along a temperature gradient.

Compared to other global transport models, such as the CliMoChem [103], the MPI-MCTM [104,105] and the 1D-POP-AS model, the Globo-POP model [12] has some limitations in studying the global fractionation. These limitations arise from two reasons. Firstly, this model only considers the latitudinal compositional shifts of POPs since the zones used were defined according to the latitude. Consequently, the model only focuses on composition shifts along the latitudinal transect. Secondly, the latitudinal transect and temperature gradient coincide closely, as shown in the case from the southern UK to northern Norway (Fig. 7) [27]. Thus, the Globo-POP model encounters difficulty separately investigating the effects of latitudinal transect and temperature gradient on POP transport.

7. Discussion

7.1. Relationship between distribution and fractionation

Fractionation has sometimes been mixed up with the distribution of POPs in the surface soil. Distributions usually refer to the concentrations in a medium observed individually for single chemical, such as a PCB congener, or a group of chemicals treated as a unit, such as a homolog. Two important kinds of distributions exist: primary and secondary distributions (See in [Section 3](#)). Fractionation is a process of composition change among several congeners or homologs during transport. Similar to distribution, primary and secondary are two important kinds of fractionations (See [Section 4](#)). From this point of view, some statements in the literature are not properly expressed. For example, the increasing trend of tetra-PCB [73] and CB-28 [98] along latitude represents a pattern of latitudinal distribution rather than latitudinal fractionation, since fractionation cannot exist for a single homolog or congener.

7.2. Global fractionation

The pioneering work by Wania and Mackay has greatly contributed to understanding the transport of POPs to the Arctic [34,41]. Global or latitudinal fractionation was introduced to address the different transport efficiencies or long-range transport potentials for several chemicals (e.g., in a suite of PCB congeners or homologs). According to the authors, global or latitudinal fractionation contains two major elements: latitudinal transect and airborne temperature gradient, which were treated as undistinguishable (See [Section 6](#)).

Latitudinal transect and airborne temperature gradient are two different mechanisms. According to a previous study [103], the latitudinal transect belongs to the differential removal hypothesis, and the airborne temperature gradient belongs to the global distillation hypothesis. Translating to our terminologies, the former is the primary factor determining the primary distribution pattern and fractionation, and the latter is the second factor determining the secondary distribution pattern and fractionation, as discussed in the previous sections.

In our opinion, global fractionation can be either primary or secondary, and the primary does not necessarily occur along latitude or temperature gradient. The monitoring data for PCBs in background soil from the southern UK to northern Norway spanning latitudes from 50.6° to 75.0° N [27], which has been

considered good evidence for latitudinal/global fractionation in soils. It revealed a primary pattern during the sampling year; thus, the air temperature did not play a major role in forming the fractionation, despite the observed correlation between the soil concentration and air temperature. In addition, global fractionation is not limited to the latitudinal direction alone, fractionation along the longitudinal transect can also be classified as a form of global fractionation. A similar longitudinal fractionation found for PCBs in Chinese background/rural soil spanning several thousand kilometers from 122° to 80° E is also a primary fractionation [28], where no temperature gradient was present. These two fractionations are identical, as discussed in [Sections 4.1.3](#) and [4.1.4](#). The major difference lies in the potential for latitudinal fractionation to develop into secondary fractionation, whereas longitudinal fractionation cannot, as shown in the animation (Animation_PCB28&180.gif) introduced in [Section 6](#).

Our study proposes that the remoteness leads to fractionation, and the temperature gradient leads to cold trapping. The decreasing temperature trend along the latitude is not the major reason for the POPs fractionating into the Polar ecosystems. The primary fractionation can bring the POPs into the polar regions, whereas the secondary fractionation can keep the POPs in the polar regions higher and longer than the non-polar regions due to the polar cold trapping mechanisms.

7.3. Polar and mountain cold trappings

A POP is polar cold trapped only when it displays a secondary latitudinal distribution pattern in a surface medium, such as soil, water, or snow. Specifically, this pattern is observed as the POPs transition from outside the Pole to inside the Pole, where the temperatures are colder, or when their concentrations in the surface medium of the Pole are higher than in the same medium in lower latitudes outside the Pole, where the temperatures are warmer [34]. An excellent example of polar cold trapping is the secondary distribution of α -HCH in seawater from the South Pacific Ocean to the Arctic Ocean during the late 1980s and early 1990s [34,106]. Similarly, the concept of mountain cold trapping, as defined by Westgate and Wania [95], refers to the higher concentrations of a POP in a surface medium at the top of the mountain than in lower sections. Thus, polar and mountain cold trappings are appreciably associated with the secondary distribution.

Mountains with different local conditions are able to cold-trap different pollutants [95]. Taking PCBs in soil as examples, both LMW- and HMW-PCBs can be mountain cold-trapped under certain conditions (See [Section 5](#)). However, the case for polar cold trapping is different. Based on the analysis of the monitoring data and the outcomes of the models described in the previous sections, we speculate that only a small number of LMW POPs, such as α -HCH, β -HCH, CB-28, and BDE-28, can form the secondary distribution pattern in soil. Many other POPs with higher K_{OA} are prone to stay in the source region or the regions close to the sources and cannot produce higher concentrations within the Poles. For example, in 1998, more than two decades after the phase-out of PCBs, a survey of PCBs in global background surface soils revealed that most (>80%) of the PCB burden in the global background surface soil still remained in the GSR [107] ([Fig. S15](#)). Another convincing evidence is the modeled distribution of CB-180 in soil by Wania and Su [12], indicating that even after 70 years since the first emission of this compound, the concentration pattern of CB-180 was still within the GSR, similar to the initial primary emission pattern. The results produced by our 1D-POP-AS Model, as shown in the animation introduced in [Section 6](#), also suggests that CB-180 cannot form the secondary distribution pattern in 80 years after their primary emission stopped, even along the latitudinal transect following a

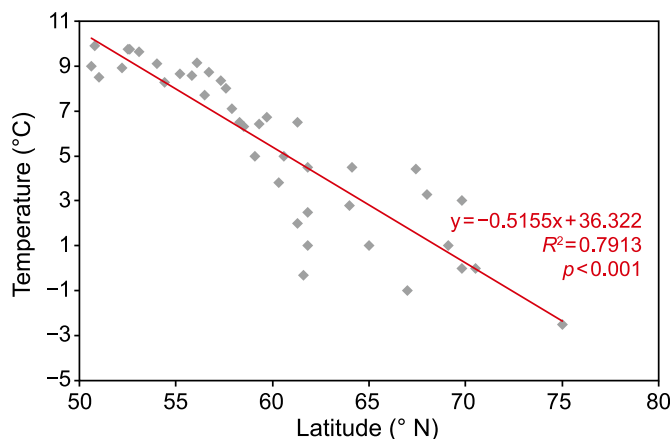


Fig. 7. Strong and significant correlation between temperature and latitude from the southern UK to northern Norway. Data are taken from Meijer et al. [27].

temperature gradient. Conversely, CB-28 demonstrates the capability to form such a secondary distribution pattern. The reason is probably that HMW PCBs have a more efficient deposition rate, less soil degradation, and stronger retention by soil organic matter. Consequently, these factors contribute to a reduced re-volatilization from soil [27,42,101–103,107]. Therefore, as the secondary factor, the temperature gradient cannot reverse the primary distribution to the secondary distribution for these chemicals.

7.4. Study for primary and secondary distributions and fractionations

It is not difficult to observe the point and urban pile and fractionations. Taking PCBs in soil as an example, for the concentration data originating from a strong point source or an urban center, without any strong point or urban source nearby, the correlation between PCB concentrations versus the distances away from the point source or urban center may be carried out. This correlation analysis can be followed by comparing the compositions of the PCB congeners or homologs. An excellent illustration of urban fractionation of PCBs in the soil is presented in Section 4.1.2, which focuses on Shanghai, China.

The monitoring program targeting the latitudinal and longitudinal fractionations presents unique challenges due to its large scale and various factors affecting the distribution and fractionation of the targeted chemicals. A few conditions for a satisfactory monitoring program for observing a longitude or latitude fractionation should be considered. First, the sampling site should be under common environmental and climatic conditions. Taking the longitudinal fractionation of PCBs in Chinese soil discussed in Section 4.1.3 as an example, the PCB levels at the sampling sites were more affected by the “local” emissions of PCBs within China, and the input PCBs through LRAT outside China were minor. Regarding the latitude fractionation in the soil from the southern UK to northern Norway discussed in Section 4.1.4, the sampling sites in the UK and Norway did not share the common environmental and climatic conditions since these two countries are separated by the North Sea. Therefore, the latitudinal fractionation pattern displayed in Norway is much better than in both countries, as revealed in Section 4.1.4. Actually, PCB soil concentrations in the UK were neither strongly nor significantly linked with latitude ($R^2 = 0.0017$ and $p = 0.83$) and longitude ($R^2 = 0.0915$ and $p = 0.18$) (Fig. S16). The same results have been observed by Heywood et al. [108], who measured the PCBs and PAHs in rural soils across the UK. Second, the monitoring sites should be on lowlands to avoid the effect of mountain cold trapping. Third, during the monitoring study, the monitoring transects should be chosen from a strong emission source or sources to remote areas (thus called remoteness). For example, Miejer et al. [27] conducted a latitude fractionation study from southern Norway with strong PCB emission sources to the remote Arctic, while Ren et al. [28] undertook a longitudinal fractionation study from eastern China with strong PCB sources to western China with much fewer PCB emissions. The strong and significant correlation between PCB concentrations and latitude or longitude ensures that the common environmental conditions or all sites can share the influence by the same source or sources of pollutants to some extent.

Several monitoring programs failed to meet the above conditions. For instance, Wang et al. [73] conducted a study on soil samples collected from the highlands (the Qingzang Plateau), spanning latitudes from 28.2° to 37.1° N and altitudes from 1920 to 5226 m above sea level [73]. Therefore, the latitudinal conditions of this study might not be deemed satisfactory, and the impact of altitudinal differences cannot be ignored. Additionally, a noteworthy observation stems from a monitoring campaign carried out

in 2012 and 2013, investigating PCB levels in forest soils across 30 mountains across China, with a latitude range of 21°–53° N and an altitude of 200–3800 m [90]. A progressive decline of relative abundance was observed with increasing latitude for tri- and tetra-PCBs, while the opposite trend was for penta- and hexa-congeners. This PCB fractionation pattern contradicts the previous findings from global-scale surveys conducted by Meijer et al. [27], which was considered to conflict with that expected from the global fractionation theory [34,41]. Actually, for the same reason discussed above, these two studies do not have comparability [73], since the findings of the latter study [90] could be caused by the combined latitudinal (from 21° to 53° N) and altitudinal (from 200 to 3800 m) factors.

Aichner and co-workers [109] analyzed PCB and PAH soil concentrations in different cities and towns in eight countries (Kathmandu in Nepal, Bangkok in Thailand, Uberlândia in Brazil, Beijing in China, some cities in Romania, several towns in France, Bayreuth and Hamburg in Germany, and Stockholm in Sweden) reported in different years (from 1998 to 2007) by different groups. They indicated a visible, increasing trend of these two groups of chemicals with latitudes. Based on this founding, the authors concluded that these concentrations in the different cities and towns fitted well into a global distribution pattern due to global distillation. However, we find this conclusion unconvincing due to several overlooked factors. Firstly, the sampling sites were located in different cities and towns far apart. Secondly, the samples were taken for different years, which did not share a common source or sources. In this case, the local sources in each city or town could play a major role. Thus, the soil pollution levels in these cities/towns with high concentrations in higher latitude regions and lower ones in the lower latitude regions were most likely due to factors other than global distillation, particularly the local sources.

7.5. Fractionations under equilibrium and steady-state P/G partitioning theory

As discussed in the previous sections, the partitioning between gaseous and particulate POPs determines the relative portions of the POPs in the gas and particle phases. Thus, it controls all the processes involved in the transfer of POPs from air to soil. Therefore, a correct description of the P/G partitioning of SVOCs in the atmosphere is critical for understanding the fractionation and long-range transport of SVOCs [42–44]. As introduced in Section 2.2, there are two different P/G partitioning equations: one is a group of equilibrium equations, represented by the Harner-Bidleman Equation, given by equation (2); and the other is the steady-state based Li-Ma-Yang Equation, given by equation (1). Here, we use BDE-28 and BDE-209 to discuss the fractionation and distribution patterns predicted by different P/G partitioning theories to make this comparison more instructive.

The different ranges of $\log K_{OA}$ for BDE-28 and BDE-209 at temperatures from –30 to 30 °C are presented in Fig. S4. For BDE-28, the $\log K_{OA}$ values range from 9.3 to 12.8, for BDE-209, they range from 14.7 to 20.7. These results indicate that within this temperature range, BDE-28 primarily exists in the EQ and NE Domains, whereas BDE-209 is entirely in the MP Domain, with a constant $\log K_{PSM}$ value of –1.53 [61]. As shown in Fig. S17(a1), for BDE-28, $\log K_p$ values predicted by the equilibrium and steady-state equations are similar in the EQ Domain, start to separate in the NE Domain, and differentiate by more than one order of magnitude in the MP Domain. For BDE-209, as shown in Fig. S17(b1), the difference is clearly discernible, from more than three orders of magnitude at 30 °C to more than nine at –30 °C. Fig. S17(a2) and (b2) depict the particle fractions for BDE-28 and BDE-209, respectively, assuming $TSP = 50 \mu\text{g m}^{-3}$. In the MP domain, the particle fractions

are estimated from 57.5% to 58.6% by the steady-state equation, while from 94.4% to 97.5% by the equilibrium equation for BDE-28; and for BDE-209, 59.5% by the steady-state equation, while 100% by the equilibrium equation. Thus, the different P/G partitioning predicted by the two equations will lead to distinct distribution and fractionation patterns. The steady-state P/G partition theory suggests similar distribution and fractionation processes for BDE-209 to BDE-28, although with less gaseous fractions. According to the equilibrium P/G partitioning theory, however, the only processes between air and soil for BDE-209 are particle wet and dry depositions with no air–soil exchange and no environmental cycling. Therefore, the BDE-209 grasshopper cannot jump, and the source region is its destination, which is inconsistent with monitoring data.

7.6. Fractionations in other media

Although this study focuses on POPs in soil in the study, it is beneficial to briefly discuss POPs in other media to broaden our perspectives in understanding fractionation. As observed in soil, the fractionation phenomenon can also occur in other media, such as air, water, and biota. Several groups have reported the fractionation phenomenon in the air [15,30,110,111]. For example, secondary fractionation over altitudinal scales has been observed in the atmosphere [15,30,110,111]. In the mountains of western Canada, some airborne OCP concentrations were reported to increase with altitude in the air at four sites along an altitudinal transect in the Canadian Rocky Mountains [110,111]. Secondary distribution patterns in the air occurred for α -HCH, β -HCH, α -endosulfan, hexachlorobenzene, and pentachlorobenzene [111].

The ocean provides the circumstances for secondary fractionation. It has been found that α -HCH in surface water of the Pacific and the Western Arctic Ocean provided an excellent example of the cold trapping and the secondary distribution pattern, where surface water concentrations increase with latitude (Fig. 8). The spatial distribution of β -HCH in the same surface ocean water differed from that of α -HCH. Whereas α -HCH steadily increased with latitude along a transect from the South Pacific Ocean to the North Pole, β -HCH also increased with latitude in the Pacific Ocean and peaked in the Bering–Chukchi region, displaying a secondary distribution pattern. However, in the Western Arctic Ocean, north of the Bering Strait, concentrations of β -HCH showed a primary distribution pattern decreasing with latitude, caused by the major transport pathway to the Arctic being ocean currents, rather than atmospheric transport [106]. Therefore, α -HCH and β -HCH

displayed a secondary fractionation pattern in both the Pacific Ocean with two secondary distribution patterns for α -HCH and β -HCH and the Arctic Ocean with the secondary distribution pattern for α -HCH and the primary distribution pattern for β -HCH, as depicted in Fig. 8.

It is interesting to note that PCBs in biota can also reflect secondary distribution and fractionation patterns. The composition of PCB homologs in the liver of a burbot (*Lota lota*) (normalized with respect to the mean value) showed a function of northern latitude along a transect through Canada [112]. While the HMW PCBs (penta-to nona-CBs) showed declining concentrations towards the north, with the rate of decrease appearing to be strongly related to the degree of chlorination (primary distribution pattern), the level of trichlorobiphenyls seems to increase with northern latitude, shown in a secondary distribution pattern. These findings demonstrate a secondary fractionation pattern in the distribution of PCBs.

8. Conclusions and prospect

The distribution pattern and fractionation of POPs have been studied by scientists in field measurements and modeling research for decades. The important knowledge derived from these researches and the present study that we know include:

- (1) During initial emissions of POPs to the atmosphere, a pulse distribution, or the primary distribution pattern, can be formed in the soil near the source. Accumulation in the soil creates secondary sources.
- (2) Over time, continuous emissions of POPs result in their dispersal in the soil, creating a distinct primary distribution pattern that extends in all directions from the pollution source. This primary distribution pattern gradually undergoes fractionation, exhibiting various forms such as point, urban, longitudinal, and latitudinal fractionations. The primary fractionation pattern is mainly caused by the primary factors, including the differential capacities of different compounds to bring the POPs from air to soil and the ability to retain POPs in the soil as a function of travel distance (or remoteness). It can be formed in all directions, including latitudinal and longitudinal transects.
- (3) The formation of the secondary distribution and fractionation patterns for POPs may need a long time after their primary emission stops. At this point, the secondary factors (air temperature, in particular) play a major role in affecting the distribution of POPs.
- (4) Global fractionations include latitudinal and longitudinal fractionations.
- (5) Latitudinal transect and airborne temperature gradient are two different mechanisms. The latitudinal transect is the primary factor determining the primary distribution pattern and fractionation, and the airborne temperature gradient is the second factor determining the secondary distribution pattern and fractionation.
- (6) The primary fractionation is the major reason for POPs to be fractionated into the polar surface media, whereas the decreasing temperature gradient along the latitude prompts the longer-term accumulation of POPs in cold polar regions (polar cold trapping).
- (7) Secondary distribution and fractionation patterns observed along increasing mountain altitudes are characterized not only by an enrichment of light POPs and depletion of heavy POPs but by an enrichment of heavy POPs and depletion of light POPs as well.

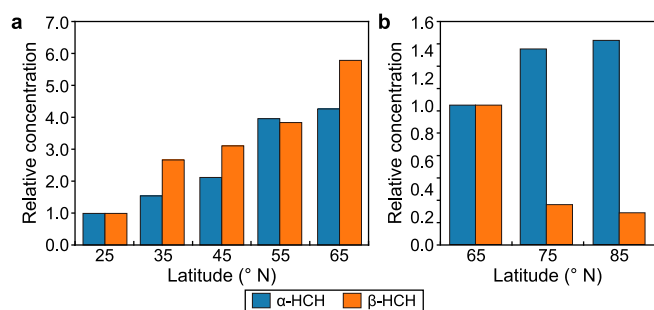


Fig. 8. The relative concentrations of α -HCH and β -HCH in the surface water of the Pacific Ocean (a) and the Western Arctic Ocean (b) measured between 1988 and 1999. Although these data span ten years and are collected from a wide range of latitudes, they illustrate well the general increase in α -HCH in cool, northern waters with exceptionally high values under the pack ice of the Canada Basin in contrast to β -HCH, which shows the highest concentrations centered on the Bering Strait ($\sim 65^\circ$ N). Data are taken from Li et al. [106].

- (8) Both the polar and mountain cold trappings are appreciably associated with the secondary distribution.

By exploring the differential behavior of POPs based on their physicochemical properties, this study aims to improve our understanding of distribution and fractionation processes associated with specific compounds in the environment. However, additional research is needed to validate and expand upon these postulations and further unravel the complex dynamics of POPs in various environmental compartments.

In the current study, it is hypothesized that not all POPs can exhibit a secondary distribution pattern in surface soil or be effectively polar cold trapped. Instead, the proposal suggests that only a limited number of relatively lighter POPs such as α -HCH, β -HCH, CB-28, and BDE-28 are capable of producing a secondary distribution pattern in the surface soil. On the other hand, POPs with higher K_{OA} may not exhibit this secondary distribution pattern. If our hypothesis is true, it would be necessary to develop a method for selecting the POPs capable of undergoing polar cold trapped (PCT) from all POPs and create a database for these PCT-POPs. Such an endeavor holds significant importance in safeguarding the pristine condition of our Arctic and Antarctic regions, shielding them from potential contamination by these PCT-POPs.

Credit authorship contribution statement

Yi-Fan Li: Conceptualization, Funding Acquisition, Project Administration, Supervision, Writing - Original Draft, Writing - Review & Editing, Visualization. **Shuai Hao:** Investigation, Data Curation, Visualization, Writing - Review & Editing. **Wan-Li Ma:** Funding Acquisition, Project Administration, Supervision, Writing - Review & Editing. **Pu-Fei Yang:** Investigation, Data Curation, Visualization, Writing - Review & Editing. **Wen-Long Li:** Investigation, Visualization, Writing - Review & Editing. **Zi-Feng Zhang:** Investigation, Writing - Review & Editing. **Li-Yan Liu:** Investigation, Writing - Review & Editing. **Robie W. Macdonald:** Conceptualization, Writing - Review & Editing.

Declaration of competing interests

The authors declare that they have no known competing financial interests or personal relationships that could have appeared to influence the work reported in this paper.

Acknowledgements

This work was supported by the National Natural Science Foundation of China (42077341), the State Key Laboratory of Urban Water Resource and Environment, Harbin Institute of Technology (No. 2022TS05), and the Special Project for Sustainable Development Science Technology in Shenzhen (No. KCXFZ20201221173000001). This study was partially supported by the Heilongjiang Touyan Innovation Team Program and the Natural Science Foundation of Heilongjiang Province of China (Grant No. LH2021E096), China. We would also like to thank the four anonymous reviewers for their valuable comments.

Appendix A. Supplementary data

Supplementary data to this article can be found online at <https://doi.org/10.1016/j.ese.2023.100311>.

References

- [1] Y.F. Li, M.T. Scholtz, B.J. van Heyst, Global gridded emission inventories of α -

- hexachlorocyclohexane, *J. Geophys. Res.* 105 (D5) (2000) 6621–6632.
- [2] Y.F. Li, M.T. Scholtz, B.J. van Heyst, Global gridded emission inventories of β -hexachlorocyclohexane, *Environ. Sci. Technol.* 37 (16) (2003) 3493–3498.
- [3] K. Breivik, A. Sweetman, J.M. Pacyna, et al., Towards a global historical emission inventory for selected PCB congeners – a mass balance approach 1. global production and consumption, *Sci. Total Environ.* 290 (1–3) (2002) 181–198.
- [4] K. Breivik, A. Sweetman, J.M. Pacyna, et al., Towards a global historical emission inventory for selected PCB congeners — a mass balance approach: 2. Emissions, *Sci. Total Environ.* 290 (1–3) (2002) 199–224.
- [5] K. Breivik, A. Sweetman, J.M. Pacyna, et al., Towards a global historical emission inventory for selected PCB congeners — a mass balance approach 3. An update, *Sci. Total Environ.* 377 (2–3) (2007) 296–307.
- [6] L. Becker, M. Scheringer, U. Schenker, et al., Assessment of the environmental persistence and long-range transport of endosulfan, *Environ. Pollut.* 159 (6) (2011) 1737–1743.
- [7] H. Shen, Y. Huang, R. Wang, et al., Global atmospheric emissions of polycyclic aromatic hydrocarbons from 1960 to 2008 and future predictions, *Environ. Sci. Technol.* 47 (12) (2013) 6415–6424.
- [8] G. Abbasi, L. Li, K. Breivik, Global historical stocks and emissions of PBDEs, *Environ. Sci. Technol.* 53 (11) (2019) 6330–6340.
- [9] R.W. Macdonald, L.A. Barrie, T.F. Bidleman, et al., Contaminants in the Canadian Arctic: 5 years of progress in understanding sources, occurrence and pathways, *Sci. Total Environ.* 254 (2–3) (2000) 93–234.
- [10] Y.F. Li, R.W. Macdonald, Sources and pathways of selected organochlorine pesticides to the Arctic and the effect of pathway divergence on HCH trends in biota: a review, *Sci. Total Environ.* 342 (1–3) (2005) 87–106.
- [11] R. Lohmann, K. Breivik, J. Dachs, et al., Global fate of POPs: current and future research directions, *Environ. Pollut.* 150 (1) (2007) 150–165.
- [12] F. Wania, Y. Su, Quantifying the global fractionation of polychlorinated biphenyls, *J. Human Environ.* 33 (3) (2004) 161–168.
- [13] S. Harrad, S. Hunter, Concentrations of polybrominated diphenyl ethers in air and soil on a rural urban transect across a major UK conurbation, *Environ. Sci. Technol.* 40 (15) (2006) 4548–4553.
- [14] A. Jamshidi, S. Hunter, S. Hazrati, et al., Concentrations and chiral signatures of polychlorinated biphenyls in outdoor and indoor air and soil in a major U.K. Conurbation, *Environ. Sci. Technol.* 41 (7) (2007) 2153–2158.
- [15] T. Harner, M. Shoeib, M. Diamond, et al., Using passive air samplers to assess urban-rural trends for persistent organic pollutants. 1. Polychlorinated biphenyls and organochlorine pesticides, *Environ. Sci. Technol.* 38 (17) (2004) 4474–4483.
- [16] T. Harner, M. Shoeib, M. Diamond, et al., Passive sampler derived air concentrations of PBDEs along an urban-rural transect: spatial and temporal trends, *Chemosphere* 64 (2) (2006) 262–267.
- [17] S. Newton, U. Sellstroem, C. Wit, Emerging flame retardants, PBDEs, and HBCDDs in indoor and outdoor media in Stockholm, Sweden, *Environ. Sci. Technol.* 49 (5) (2015) 2912–2920.
- [18] W. Wilcke, M. Krauss, G. Safronov, et al., Polychlorinated biphenyls (PCBs) in soils of the Moscow region: concentrations and small-scale distribution along an urban-rural transect, *Environ. Pollut.* 141 (2) (2006) 327–335.
- [19] J. Liu, W. Liu, Distribution of polychlorinated dibenzo-p-dioxins and dibenzofurans (PCDDs/Fs) and dioxin-like polychlorinated biphenyls (dioxin-like PCBs) in the soil in a typical area of eastern China, *J. Hazard Mater.* 163 (2–3) (2009) 959–966.
- [20] D.G. Wang, M. Yang, Q.I. Hong, et al., An Asia-specific source of dechlorane plus: concentration, isomer profiles, and other related compounds, *Environ. Sci. Technol.* 44 (17) (2010) 6608–6613.
- [21] W. Liu, H. Li, Z. Tian, et al., Spatial distribution of polychlorinated biphenyls in soil around a municipal solid waste incinerator, *J. Environ. Sci.* 25 (8) (2013) 1636–1642.
- [22] Y.-F. Zhang, S. Fu, Y. Dong, et al., Distribution of polychlorinated biphenyls in soil around three typical industrial sites in Beijing, China, *Bull. Environ. Contam. Toxicol.* 92 (4) (2014) 466–471.
- [23] J. Wang, L. Liu, J. Wang, et al., Distribution of metals and brominated flame retardants (BFRs) in sediments, soils and plants from an informal e-waste dismantling site, South China, *Environ. Sci. Pollut. Control Ser.* 22 (2) (2014) 1020–1033.
- [24] W.L. Li, L.Y. Liu, Z.F. Zhang, et al., Brominated flame retardants in the surrounding soil of two manufacturing plants in China: occurrence, composition profiles and spatial distribution, *Environ. Pollut.* 213 (2016) 1–7.
- [25] J.-h. Zhang, Z. Zhang, G.-h. Chen, Distribution of polychlorinated biphenyls and polybrominated diphenyl ethers in soils of a previous E-waste processing center, *Toxicol. Environ. Chem.* 98 (2) (2016) 204–215.
- [26] T.J. McGrath, P.D. Morrison, A.S. Ball, et al., Spatial distribution of novel and legacy brominated flame retardants in soils surrounding two Australian electronic waste recycling facilities, *Environ. Sci. Technol.* 52 (15) (2018) 8194–8204.
- [27] S.N. Meijer, E. Steinnes, W.A. Ockenden, et al., Influence of environmental variables on the spatial distribution of PCBs in Norwegian and U.K. soils: implications for global cycling, *Environ. Sci. Technol.* 36 (10) (2002) 2146–2153.
- [28] N. Ren, M. Que, L.I. Yi-Fan, et al., Polychlorinated biphenyls in Chinese surface soils, *Environ. Sci. Technol.* 41 (11) (2007) 3871–3876.
- [29] P. Ružičková, J. Klánová, P. Čupr, et al., An assessment of air-soil exchange of polychlorinated biphenyls and organochlorine pesticides across central and

- southern Europe, *Environ. Sci. Technol.* 42 (1) (2008) 179–185.
- [30] S.N. Meijer, Ockenden, et al., Spatial and temporal trends of POPs in Norwegian and UK background air: implications for global cycling, *Environ. Sci. Technol.* 37 (3) (2003) 454–461.
- [31] W.L. Li, W.L. Ma, H. Jia, et al., Polybrominated diphenyl ethers (PBDEs) in surface soils across five Asian countries: levels, spatial distribution and source contribution, *Environ. Sci. Technol.* 50 (23) (2016) 12779–12788.
- [32] W.L. Li, W.L. Ma, Z. Zhang, et al., Occurrence and Source Effect of Novel Brominated Flame Retardants (NBFRs) in Soils from Five Asian Countries and its Relationship with PBDEs, vol. 51, *Environmental Science & Technology*, 2017, pp. 11126–11135.
- [33] D. Mackay, F. Wania, Global fractionation and cold condensation of low volatility organochlorine compounds in polar regions, *AMBIO A J. Hum. Environ.* 22 (1) (1993) 10–18.
- [34] Wania, Frank, Mackay, et al., Tracking the distribution of persistent organic pollutants, *Environ. Sci. Technol.* 30 (9) (1996) 390–396.
- [35] W.D. Lead, Polychlorinated biphenyls in UK and Norwegian soils: spatial and temporal trends, *Sci. Total Environ.* 193 (3) (1997) 229–236.
- [36] C. Agrell, L. Okla, P. Larsson, et al., Evidence of latitudinal fractionation of polychlorinated biphenyl congeners along the Baltic sea region, *Environ. Sci. Technol.* 33 (8) (1999) 1149–1156.
- [37] W.A. Lead, E. Steinnes, K.C. Jones, Atmospheric deposition of PCBs to moss (*Hylocomium splendens*) in Norway between 1977 and 1990, *Environ. Sci. Technol.* 30 (2) (1996) 524–530.
- [38] A. Bignert, M. Olsson, W. Persson, et al., Temporal trends of organochlorines in Northern Europe, 1967–1995. Relation to global fractionation, leakage from sediments and international measures, *Environ. Pollut.* 99 (2) (1998) 177–198.
- [39] Y.F. Li, T. Harner, L. Liu, et al., Polychlorinated biphenyls in global air and surface soil: distributions, air-soil exchange, and fractionation effect, *Environ. Sci. Technol.* 44 (8) (2010) 2784–2790.
- [40] L.Y. Liu, W.L. Ma, H.L. Jia, et al., Research on persistent organic pollutants in China on a national scale: 10 years after the enforcement of the Stockholm Convention, *Environ. Pollut.* 217 (2016) 70–81.
- [41] F. Wania, D. Mackay, Global fractionation and cold condensation of low volatility organochlorine compounds in polar regions, *J. Human Environ.* 22 (1993) 10–18.
- [42] M. Scheringer, Analyzing the Global Fractionation of Persistent Organic Oollutants (POPs), *Nato Security Through Science*, 2008, pp. 189–203.
- [43] M.D. Cohen, R.R. Draxler, R. Artz, et al., Modeling the atmospheric transport and deposition of PCDD/F to the great lakes, *Environ. Sci. Technol.* 36 (22) (2002) 4831–4845.
- [44] M. Scheringer, F. Wania, *Multimedia Models of Global Transport and Fate of Persistent Organic Pollutants*, vol. 30, Springer Berlin Heidelberg, 2003, pp. 237–269.
- [45] F. Wania, J.N. Westgate, On the mechanism of mountain cold-trapping of organic chemicals, *Environ. Sci. Technol.* 42 (24) (2008) 9092–9098.
- [46] C.W. GÖtz, M. Scheringer, M. Macleod, et al., Alternative approaches for modeling gas-particle partitioning of semivolatile organic chemicals: model development and comparison, *Environ. Sci. Technol.* 41 (4) (2007) 1272–1278.
- [47] P. Shahpoury, G. Lammel, A. Albinet, et al., Evaluation of a conceptual model for gas-particle partitioning of polycyclic aromatic hydrocarbons using polyparameter linear free energy relationships, *Environ. Sci. Technol.* 50 (22) (2016) 12312–12319.
- [48] J.F. Pankow, Review and comparative-analysis of the theories on partitioning between the gas and aerosol particulate phases in the atmosphere, *Atmos. Environ.* 21 (11) (1987) 2275–2283.
- [49] L.N. Qiao, P.T. Hu, R. Macdonald, et al., Modeling gas/particle partitioning of polybrominated diphenyl ethers (PBDEs) in the atmosphere: a review, *Sci. Total Environ.* 729 (20) (2020) 138962.
- [50] M. Hippelein, M.S. McLachlan, Soil/air partitioning of semivolatile organic compounds. 1. method development and influence of physical-chemical properties, *Environ. Sci. Technol.* 32 (2) (1998) 310–316.
- [51] T. Harner, T.F. Bidleman, L.M.M. Jantunen, et al., Soil-air exchange model of persistent pesticides in the United States cotton belt, *Environ. Toxicol. Chem.* 20 (7) (2001) 1612–1621.
- [52] A. Hassani, K. Breivik, S.N. Meijer, et al., PBDEs in European background soils: levels and factors controlling their distribution, *Environ. Sci. Technol.* 38 (3) (2004) 738–745.
- [53] T.E. Bidleman, A. Leone, Soil-air relationships for toxaphene in the southern United States, *Environ. Toxicol. Chem.* 23 (10) (2004) 2337–2342.
- [54] A. Bozlaker, M. Odabasi, A. Muezzinoglu, Dry deposition and soil-air gas exchange of polychlorinated biphenyls (PCBs) in an industrial area, *Environ. Pollut.* 156 (3) (2008) 784–793.
- [55] G.L. Daly, Y.D. Lei, C. Teixeira, et al., Pesticides in western Canadian mountain air and soil, *Environ. Sci. Technol.* 41 (17) (2007) 6020–6025.
- [56] D.S. Drage, S. Newton, C.D. Wit, et al., Concentrations of legacy and emerging flame retardants in air and soil on a transect in the UK West Midlands, *Chemosphere* 148 (2016) 195–203.
- [57] D. Mackay, L.S. Mccarty, M. Macleod, On the validity of classifying chemicals for persistence, bioaccumulation, toxicity, and potential for long-range transport, *Environ. Toxicol. Chem.* 20 (7) (2001) 1491–1498.
- [58] F. Wong, T. Harner, Q.T. Liu, et al., Using experimental and forest soils to investigate the uptake of polycyclic aromatic hydrocarbons (PAHs) along an urban-rural gradient, *Environ. Pollut.* 129 (3) (2004) 387–398.
- [59] F. Wong, A. Henry, Alegria, et al., Organochlorine pesticides in soils and air of southern Mexico: chemical profiles and potential for soil emissions, *Atmos. Environ.* 42 (33) (2008) 7737–7745.
- [60] M. Odabasi, B. Cetin, Determination of octanol-air partition coefficients of organochlorine pesticides (OCPs) as a function of temperature: application to air-soil exchange, *J. Environ. Manag.* 113 (2012) 432–439.
- [61] Y.F. Li, W.L. Ma, M. Yang, Prediction of gas/particle partitioning of polybrominated diphenyl ethers (PBDEs) in global air: a theoretical study, *Atmos. Chem. Phys.* 15 (4) (2015) 1669–1681.
- [62] T. Harner, T.F. Bidleman, Octanol-air partition coefficient for describing particle/gas partitioning of aromatic compounds in urban air, *Environ. Sci. Technol.* 32 (10) (1998) 1494–1502.
- [63] J.F. Pankow, T.F. Bidleman, Interdependence of the slopes and intercepts from log-log correlations of measured gas-particle partitioning and vapor pressure—I. theory and analysis of available data, *Atmos. Environ., Part A* 26 (6) (1992) 1071–1080.
- [64] J.F. Pankow, T.F. Bidleman, Effects of temperature, TSP and per cent non-exchangeable material in determining the gas-particle partitioning of organic compounds, *Atmos. Environ. Part A Gen. Top.* 25 (10) (1991) 2241–2249.
- [65] M. Yang, Y.F. Li, L.N. Qiao, et al., Estimating subcooled liquid vapor pressures and octanol-air partition coefficients of polybrominated diphenyl ethers and their temperature dependence, *Sci. Total Environ.* 628 (1) (2018) 329–337.
- [66] J.G. McDonald, R.A. Hites, Radial dilution model for the distribution of toxaphene in the United States and Canada on the basis of measured concentrations in tree bark, *Environ. Sci. Technol.* 37 (3) (2003) 475–481.
- [67] Q. Zheng, L. Nizzetto, J. Li, et al., Spatial distribution of old and emerging flame retardants in Chinese forest soils: sources, trends and processes, *Environ. Sci. Technol.* 49 (5) (2015) 2904–2911.
- [68] B. Gevao, A.N. Ghabban, S. Uddin, et al., Polybrominated diphenyl ethers (PBDEs) in soils along a rural-urban-rural transect: sources, concentration gradients, and profiles, *Environ. Pollut.* 159 (12) (2011) 3666–3672.
- [69] M. Yang, H. Qi, H.L. Jia, et al., Polybrominated diphenyl ethers in air across China: levels, compositions, and gas-particle partitioning, *Environ. Sci. Technol.* 47 (15) (2013) 8978–8984.
- [70] Z.L. Zhang, C. Leith, S.M. Rhind, et al., Long Term Temporal and Spatial Changes in the Distribution of Polychlorinated Biphenyls and Polybrominated Diphenyl Ethers in Scottish Soils, vols. 468–469, *Science of The Total Environment*, 2014, pp. 158–164.
- [71] H. Jia, L. Liu, Y. Sun, et al., Monitoring and modeling endosulfan in Chinese surface soil, *Environ. Sci. Technol.* 44 (24) (2010) 9279–9284.
- [72] Z. Zhang, C. Tian, H. Jia, et al., Gridded usage inventories of polychlorinated biphenyls (PCBs) in China, *J. Nat. Sci. Heilongjiang Univ.* 27 (2010) 111–116 (in Chinese).
- [73] X.P. Wang, J.J. Sheng, P. Gong, et al., Persistent organic pollutants in the Tibetan surface soil: spatial distribution, air-soil exchange and implications for global cycling, *Environ. Pollut.* 170 (2012) 145–151.
- [74] C. Tian, L. Liu, J. Ma, et al., Modeling redistribution of α -HCH in Chinese soil induced by environment factors, *Environ. Pollut.* 159 (10) (2011) 2961–2967.
- [75] Z. Zhang, L. Liu, Y.-F. Li, et al., Analysis of polychlorinated biphenyls in concurrently sampled Chinese air and surface soil, *Environ. Sci. Technol.* 42 (17) (2008) 6514–6518.
- [76] H. Zhang, Y. Luo, Y. Teng, PCB contamination in soils of the Pearl River Delta, South China: levels, sources, and potential risks, *Environ. Sci. Pollut. Res.* 20 (8) (2013) 5150–5159.
- [77] N.L. Devi, I.C. Yadav, P. Chakraborty, et al., Polychlorinated biphenyls in surface soil from north-east India: implication for sources Apportionment and health-risk assessment, *Arch. Environ. Contam. Toxicol.* 75 (3) (2018) 377–389.
- [78] S. Cui, Q. Fu, Y.F. Li, et al., Modeling the air-soil exchange, secondary emissions and residues in soil of polychlorinated biphenyls in China, *Sci. Rep.* 7 (2045-2322) (2017) 221–230.
- [79] J.M. Blais, D.W. Schindler, D. Muir, et al., Accumulation of persistent organochlorine compounds in mountains of western Canada, *Nature* 395 (6702) (1998) 585–588.
- [80] Z.M. Migaszewski, Determining organic compound ratios in soils and vegetation of the Holy Cross Mtns., Poland., *Water, Air, Soil Pollut.* 111 (1999) 123–138.
- [81] A. Ribes, J.O. Grimalt, C.J.T. García, et al., Temperature and organic matter dependence of the distribution of organochlorine compounds in mountain soils from the subtropical Atlantic (Teide, Tenerife Island), *Environ. Sci. Technol.* 36 (9) (2002) 1879–1885.
- [82] D. Chen, W. Liu, X. Liu, et al., Cold-trapping of persistent organic pollutants in the mountain soils of western Sichuan, China, *Environ. Sci. Technol.* 42 (24) (2008) 9086–9091.
- [83] P. Tremolada, S. Villa, P. Bazzarin, et al., POPs in mountain soils from the Alps and Andes: suggestions for a 'precipitation effect' on altitudinal gradients, *Water, Air, Soil Pollut.* 188 (1-4) (2008) 93–109.
- [84] P. Wang, Q. Zhang, Y. Wang, et al., Altitude dependence of polychlorinated biphenyls (PCBs) and polybrominated diphenyl ethers (PBDEs) in surface soil from Tibetan Plateau, China, *Chemosphere* 76 (11) (2009) 1498–1504.
- [85] X. Zheng, X. Liu, G. Jiang, et al., Distribution of PCBs and PBDEs in soils along the altitudinal gradients of Balang Mountain, the east edge of the Tibetan

- Plateau, *Environ. Pollut.* 161 (2012) 101–106.
- [86] W. Meng, W. Pu, R. Yang, et al., Altitudinal dependence of PCBs and PBDEs in soil along the two sides of Mt. Sygera, southeastern Tibetan Plateau, *Sci. Rep.* 8 (1) (2018) 14307–14314.
- [87] H. Shen, Bernhard Henkelmann, Walkiria Levy, et al., Altitudinal and chiral signature of persistent organochlorine pesticides in air, soil, and spruce needles (*Picea abies*) of the Alps, *Environ. Sci. Technol.* 43 (7) (2009) 2450–2455.
- [88] A. Zhang, W. Liu, H. Yuan, et al., Spatial distribution of hexachlorocyclohexanes in agricultural soils in Zhejiang province, China, and correlations with elevation and temperature, *Environ. Sci. Technol.* 45 (15) (2011) 6303.
- [89] A. Zhang, L. Fang, J. Wang, et al., Residues of currently and never used organochlorine pesticides in agricultural soils from Zhejiang province, China, *J. Agric. Food Chem.* 60 (12) (2012) 2982–2988.
- [90] Q. Zheng, L. Nizzetto, M. Mulder, et al., Does an analysis of polychlorinated biphenyl (PCB) distribution in mountain soils across China reveal a latitudinal fractionation paradox? *Environ. Pollut.* 195 (dec) (2014) 115–122.
- [91] G. Carrera, P. Fernández, R.M. Vilanova, et al., Persistent organic pollutants in snow from European high mountain areas, *Atmos. Environ.* 35 (2) (2001) 245–254.
- [92] J.O. Grimalt, P. Fernandez, L. Berdie, et al., Selective trapping of organochlorine compounds in mountain lakes of temperate areas, *Environ. Sci. Technol.* 35 (13) (2001) 2690–2697.
- [93] Grimalt, Francesca, Joan, et al., Temperature dependence of the distribution of organochlorine compounds in the mosses of the Andean Mountains, *Environ. Sci. Technol.* 38 (20) (2004) 5386–5392.
- [94] E. Gallego, J.O. Grimalt, M. Bartrons, et al., Altitudinal gradients of PBDEs and PCBs in fish from European high mountain lakes, *Environ. Sci. Technol.* 41 (2007) 2196–2202.
- [95] J.N. Westgate, F. Wania, Model-based exploration of the drivers of mountain cold-trapping in soil, *Environ.Sci. Proc. & Impacts* 15 (12) (2013) 2220–2232.
- [96] D. Calamari, E. Bacci, S. Focardi, et al., Role of plant biomass in the global environmental partitioning of chlorinated hydrocarbons, *Environ. Sci. Technol.* 25 (1991) 1489–1495.
- [97] R. Lohmann, G. Lammel, Adsorptive and absorptive contributions to the gas-particle partitioning of polycyclic aromatic hydrocarbons: state of knowledge and recommended parametrization for modeling, *Environ. Sci. Technol.* 38 (14) (2004) 3793–3803.
- [98] S. Cui, Q. Fu, C. Tian, et al., Modeling primary and secondary fractionation effects and atmospheric transport of polychlorinated biphenyls through single-source emissions, *Environ. Geochem. Health* 41 (2019) 1939–1951.
- [99] T. Gouin, D. Mackay, K.C. Jones, et al., Evidence for the "grasshopper" effect and fractionation during long-range transport of organic contaminants, *Environ. Pollut.* 128 (1-2) (2004) 139–148.
- [100] Rainer, Gerhard Lohmann, et al., Adsorptive and absorptive contributions to the gas-particle partitioning of polycyclic aromatic hydrocarbons: state of knowledge and recommended parametrization for modeling, *Environ. Sci. Technol.* 38 (14) (2004) 3793–3803.
- [101] M. Scheringer, M. Salzmann, M. Stroebe, et al., Long-range transport and global fractionation of POPs: insights from multimedia modeling studies, *Environ. Pollut.* 128 (1-2) (2004) 177–188.
- [102] I. Stemmler, G. Lammel, Long-term trends of continental-scale PCB patterns studied using a global atmosphere-ocean general circulation model, *Environ. Sci. Pollut. Res.* 19 (6) (2012) 1971–1980.
- [103] H.V. Waldow, M. Macleod, K. Jones, et al., Remoteness from emission sources explains the fractionation pattern of polychlorinated biphenyls in the northern hemisphere, *Environ. Sci. Technol.* 44 (16) (2010) 6183–6188.
- [104] V.S. Semeena, J. Feichter, G. Lammel, Impact of the regional climate and substance properties on the fate and atmospheric long-range transport of persistent organic pollutants - examples of DDT and γ -HCH, *Atmos. Chem. Phys.* 6 (5) (2006) 1231–1248.
- [105] F. Guglielmo, G. Lammel, E. Maier-Reimer, Global environmental cycling of gamma-HCH and DDT in the 1980s—a study using a coupled atmosphere and ocean general circulation model, *Chemosphere* 76 (11) (2009) 1509–1517.
- [106] Y.F. Li, R.W. Macdonald, L. Jantunen, et al., The transport of β -hexachlorocyclohexane to the western Arctic Ocean: a contrast to α -HCH, *Sci. Total Environ.* 291 (1-3) (2002) 229–246.
- [107] S.N. Meijer, W.A. Ockenden, A. Sweetman, et al., Global distribution and budget of PCBs and HCB in background surface soils: implications for sources and environmental processes, *Environ. Sci. Technol.* 37 (4) (2003) 667–672.
- [108] E. Heywood, J. Wright, C.L. Wienburg, et al., Factors influencing the national distribution of polycyclic aromatic hydrocarbons and polychlorinated biphenyls in British soils, *Environ. Sci. Technol.* 40 (24) (2006) 7629–7635.
- [109] B. Aichner, B. Glaser, W. Zech, Polycyclic aromatic hydrocarbons and polychlorinated biphenyls in urban soils from Kathmandu, Nepal, *Org. Geochem.* 38 (4) (2007) 700–715.
- [110] L. Shen, F. Wania, Y. Lei, et al., Atmospheric distribution and long-range transport behavior of organochlorine pesticides in north America, *Environ. Sci. Technol.* 39 (2) (2005) 409–420.
- [111] L. Shen, F. Wania, Y.D. Lei, et al., Hexachlorocyclohexanes in the north American atmosphere, *Environ. Sci. Technol.* 38 (4) (2004) 965–975.
- [112] D. Muir, C.A. Ford, N.P. Grift, et al., Geographic variation of chlorinated hydrocarbons in burbot (*Lota lota*) from remote lakes and rivers in Canada, *Arch. Environ. Contam. Toxicol.* 19 (4) (1990) 530–542.